10-29-2020 1:00 PM

Development and Validation of Augmented Reality Training Simulator for Ultrasound Guided Percutaneous Renal Access

Yanyu Mu, *The University of Western Ontario*

Abstract

Percutaneous renal access (PCA) is a critical step in needle-based renal procedures. Traditional PCA training relies on apprenticeship, which raises concerns about patient safety and limits training opportunities. In this thesis, we reviewed simulation-based training for PCA, described the development of a novel augmented reality (AR) simulator for ultrasound (US)-guided PCA, and evaluated its validity and efficacy as a teaching tool.

Our AR simulator allows the user to practice PCA on a silicone phantom using a tracked needle and US probe emulator under the guidance of simulated US on a tablet screen. 6 Expert and 24 novice participants were recruited to evaluate the efficacy of our simulator.

Experts highly rated the realism and usefulness of our simulator, reflected by the average face validity score of 4.39 and content validity score of 4.53 on a 5-point Likert scale. Comparisons with a Mann-Whitney U test revealed significant differences ($p<0.05$) in performances between the experts and novices on 6 out of 7 evaluation metrics, demonstrating strong construct validity. Furthermore, a paired T-test indicated significant performance improvements ($p<0.05$) of the novices in both objective and subjective evaluation after training with our simulator.

Our cost-effective, flexible, and easily customizable AR training simulator can provide opportunities for trainees to acquire basic skills of US-guided PCA in a safe and stress-free environment. The effectiveness of our simulator is demonstrated through strong face, content, and construct validity, indicating its value as a novel training tool.

Keywords: Augmented reality, Percutaneous renal access, Training simulator, Ultrasound-guided needle insertion

Summary of Lay Audience

Percutaneous renal access (PCA) is the initial step to gain access to the kidney for treating common kidney diseases such as kidney stones. At present, mastering of this technique relies on extensive clinical training. However, it is very challenging to keep up with the increasing training demand for many training centres. To lessen the burden of the clinical education and deliver safer patient care, training simulators were employed to provide supplementary training opportunities. This thesis reviewed the existing training simulators for PCA and found no augmented reality (AR)/ virtual reality (VR) simulator available for ultrasound (US)-guided PCA, which is a safer alternative to fluoroscopy (FL)-guided PCA. Therefore, the goal of this work was to develop and validate a training simulator for US-guided PCA.

Following a minimalism design approach, we integrated three-dimensional (3D) printed hardware components, an easy-to-make silicone phantom, and personal mobile device to build an low-cost training simulator for US-guided PCA. Since the surgical scene, including the the kidney and US images are simulated and visualized in AR, the tradition lab setting is no longer required. Trainees have the option to practice at home in a stress-free environment. In addition, this simulator provides performance feedback via direct visualization and data sheet, which facilitate deliberate practice without supervision. For educators, new training content, such as patient specific cases can be easily imported to this simulator without any hardware alteration.

A user study was conducted to validate some aspects of this simulator, and demonstrate that training using our simulator resulted in significant skill improvements. To incorporate this simulator into the training curriculum, more rigorous validation is required for future work.

Co-Authorship Statement

The following thesis contains one manuscript that has been published:

Mu, Y., Hocking, D., Wang, Z., Garvin, G.J., Eagleson, R. and Peters, T.M., Augmented reality simulator for ultrasound-guided percutaneous renal access. *International Journal of Computer Assisted Radiology and Surgery,* 15(5):749–757, 2020.

My contribution to this work including engineering design, programming, prototyping and testing, study design, data collection and analysis, drafting and revising the manuscript. Hocking, D. Wang, Z., and Garvin, G.J. provided clinical insight. Hocking and D. Wang Z. also aided with testing, user study and recruitment. Eagleson, R. and Peters, T.M. provided supervision on design and testing. All authors contributed editorial feedback during the manuscript review.

Acknowledgements

Firstly, I would like to thank my supervisor Dr. Terry Peters for his guidance, and continuous support. Your passion and dedication to research and education have motivated me tremendously through difficult times. You have provided me with clear advice when needed, and a lot of freedom to experiment and create. I am very grateful for the opportunity you have given me to be part of your lab and getting involved in cutting edge researches. I would like to thank my co-supervisor Dr. Roy Eagleson for his guidance and insights. I am truly grateful for your expertise and constructive feedback throughout this work.

To my advisory committee, Dr. Elvis Chen, Dr. Peter Wang, Dr. David Hocking, and Dr. Greg Garvin, thank you all for being extremely supportive and enthusiastic throughout this project. Your expertise and insights were essential to the completion of this thesis.

Thank you to the WARP group for pulling all the resources together, and provide funding for this project. I have learned a lot from each meeting. This project would not happen without this group.

I would also like to thank the past and present members of the VASST lab. It has been my privilege to work with a group of talented people. Special thanks to Wenyao Xia, I can always count on your support whenever I run into problems. You always have the solution to my questions, from stats to writing. To Yingli Lv, thank you for guiding me through programming issues which saved me a lot of time from debugging. Thank you to Adam Rankin and John Moore for your help with prototyping and technical support through out this work.

I would like to extend my gratitude to my parents, fellow graduate students, and friends from BME and Robarts who have always been there for me.

Contents

List of Figures

List of Tables

List of Abbreviations, Symbols, and Nomenclature

Terminology

3D	Three-dimensional
PCA	Percutaneous renal access
AR	Augmented reality
VR	Virtual reality
OR	Operating room
US	Ultrasound
FL	Fluoroscopy
PCNL	Percutaneous nephrolithotomy
GRS	Global rating scale
HMD	Head-mounted display
CT	Computed tomography
MRI	Magnetic resonance imaging
EMT	Electromagnetic tracking
SDK	Software development kit
STL	Stereolithography
ROI	Region of interest
DLL	Dynamic-link library
SO	Shared object

Chapter 1

Introduction

Percutaneous renal surgery is a standard minimally invasive procedure for diagnosis or treatment of a variety of renal pathologies such as kidney stones and tumors [84]. In most cases, the first step of percutaneous renal surgery is to create needle access from the skin into the kidney under ultrasound (US) or fluoroscopic (FL) guidance [75]. This initial needle access serves as a safe passage for larger surgical instruments, allowing surgeons to perform the surgery without opening layers of tissues. Compared to open renal surgeries, percutaneous procedures are less invasive and are associated with lower morbidity [43]. Nevertheless, access related complications, such as serious hemorrhage and pulmonary injuries, have been reported [47][68]. Given that the kidney is highly vascularized, and is surrounded by vital organs such as the lung and the colon, percutaneous renal access (PCA) is considered as the most challenging step during needle-based renal procedures. Thus, establishing a safe and efficient PCA is crucial to the success of percutaneous renal surgeries and the recovery of patients [46].

This chapter includes the steps taken to guide the design of a training simulator for PCA.

1. Provide a relevant clinical background of PCA, identify the technical challenges performing this procedure, and associated complications.

2. Review the current training method, identify the problem in training, and discuss potential solutions.

3. Summarize the characteristics of medical training simulators, review the existing training simulators for PCA, identify what is missing, and discuss feasible engineering solutions.

1.1 Clinical Background

1.1.1 The Early Development of PCA

The first documented PCA was performed by Thomas Hillier in 1864, to treat a 4-year-old boy with a severe hydronephrotic right kidney due to a congenital defect. Over a period of four and a half years, Hillier aspirated the boy's right kidney periodically for temporary drainage, and even attempted to establish a permanent fistula. Unfortunately, the fistula did not persist, and the boy later died of a stone that obstructed his healthy left kidney at the age of 8 [13]. As x-ray imaging and pyelography became available for visualizing the urinary system, Nils Alwall applied the liver biopsy technique on the kidney and performed the first image-guided percutaneous renal biopsy in 1944 [6][75]. Poul Iverson and Claus Brun [49] subsequently perfected this technique, and it was quickly adopted by physicians around the world for renal diagnosis. Henceforth, PCA techniques were adopted for the treatment of many urological diseases, such as kidney stones and tumors. Improvement in techniques and advancement in equipment resulted in percutaneous renal procedures, and because of its low complication rate and lower blood loss [15], percutaneous renal procedures became the preferred treatment over open renal surgeries .

1.1.2 Image-Guidance for PCA

During minimally invasive surgeries (MIS), image-guidance is crucial to surgeons, just as navigational technology is to a pilot when flying at night [70]. Since surgeons can no longer see or feel the pathology or anatomical relationships as they could during open surgeries, this information must be provided by intraoperative real-time imaging modalities. The most com-

monly used image-guidance modalities for PCA are fluoroscopy (FL) and ultrasound (US). In addition, computed tomography (CT)-guidance may be required for patients with abnormal morphology such as morbid obesity, retrorenal colon, enlarged spleen, etc. [46].

FL has been used as the primary imaging modality for PCA guidance, as it provides high-resolution imaging of the collecting system and good visibility of small stone fragments, needle, and guidewire [46][48]. However, cumulative radiation exposure to patients and providers during FL-guided PCA poses an increased health risk [97], while the long term effect of low-dose ionizing radiation is still being investigated [18][62].

Compared to FL, US has the advantage of imaging of the visceral organs surrounding the kidney in real time, eliminating the need for contrast material, and provides comparable surgical outcomes at a lower institutional cost. Above all, US-guidance is radiation free, hence ideal for pregnant women and children [34][97]. Disadvantage of US-guidance including the lack of anatomic details, limited visualization of the guidewire, and difficulty tracking of small stone fragments (Figure 1.1) [46][48].
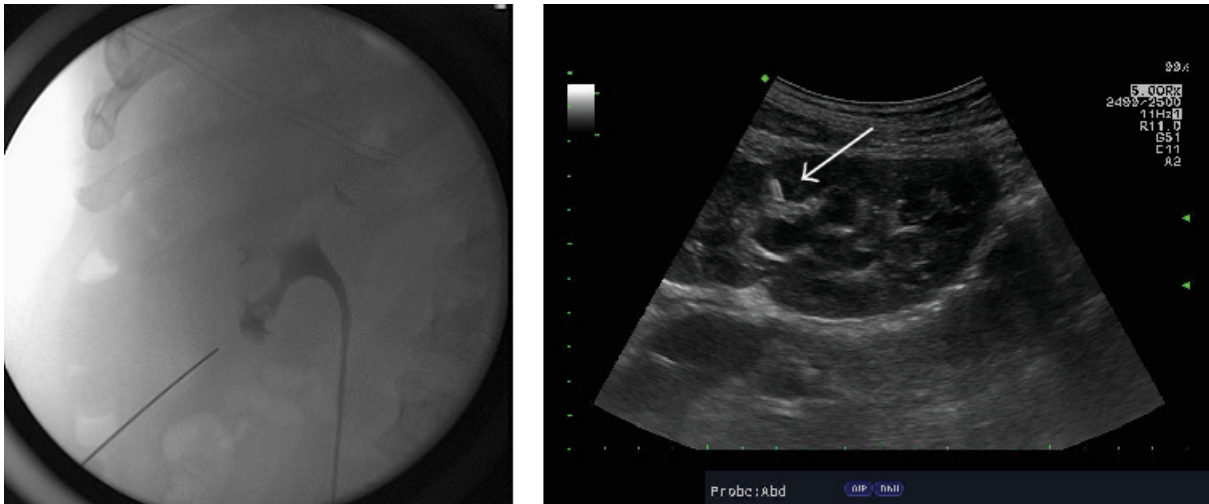
Figure 1.1: FL-guided PCA (Left) [86] vs US guided PCA(Right) [16]. Image used with the permission of Mary Ann Liebert Inc. and Hindawi.
.

A number of studies comparing clinical outcomes of percutaneous nephrolithotomy (PCNL) using US or FL guided access found no significant differences between the two groups in terms

of total operating time and success rate. Whereas the US groups had higher stone-free rate, shorter radiation exposure time, fewer access attempts, and lower incidence of hemorrhage (bleeding), the FL groups had shorter access time [2][7][12][25][38][42]. A Higher incidence of hemorrhage was found to be associated with the larger sheath size and a higher number of punctures performed during FL-guided procedures [7].

In conclusion, FL and US each have their advantages and disadvantages. While choosing an imaging modality for PCA guidance, the characteristics of each modality should be considered. Whereas US-guided PCA has gained popularity around world including China and the U.S., this technique is rarely practiced in Canada, mainly due to the lack of training [19]. As more Canadian institutions move towards adopting US-guided PCA, it is recommended to use US-guidance on patients with dilated collecting systems, and which are free of staghorn stones [12][53]. In addition, US can be used as an adjunct to FL as a strategy to reduce radiation exposure [2][110].

1.1.3   US-Guided PCA Techniques and Complications

Anatomical Considerations

While planning for the best approach to the collecting system, a solid understanding of the renal anatomy and the renal arterial system is of utmost importance for safe and efficient PCA. The kidneys are positioned between the abdominal lining and the back, defined as the retroperitoneal space. Nephrons are the filtering units of the kidney that filter the blood to regulate chemical concentration and produce urine. There are approximately one million nephrons found through out the medulla and the cortex, which is the pyramid shaped segments and the outer region of the kidney respectively. The renal pyramids project into funnel shaped chambers called calyces. The calyces are positioned radially around the renal pelvis, which is the innermost hollow centre of the kidney where urine collects. The kidneys are highly vascularized organs, with the renal artery branches into anterior and posterior divisions [39]. Between these two divisions, lies the avascular field, known as the Brödel's line (Figure 1.2) [39]. To

avoid vascular injury, the best point of entry is through the fornix into a posterior calyx, which usually traverses Brödel's line [39]. Direct puncture into the infundibulum or renal pelvis could result in significant hemorrhage. Moreover, the resulting tract would not be able to provide adequate stability for other surgical instruments such as a nephrostomy tube [53][77]. Inadvertent puncture of an anterior calyx can also lead to increased risk of bleeding and difficulty accessing the ureter [39][46].
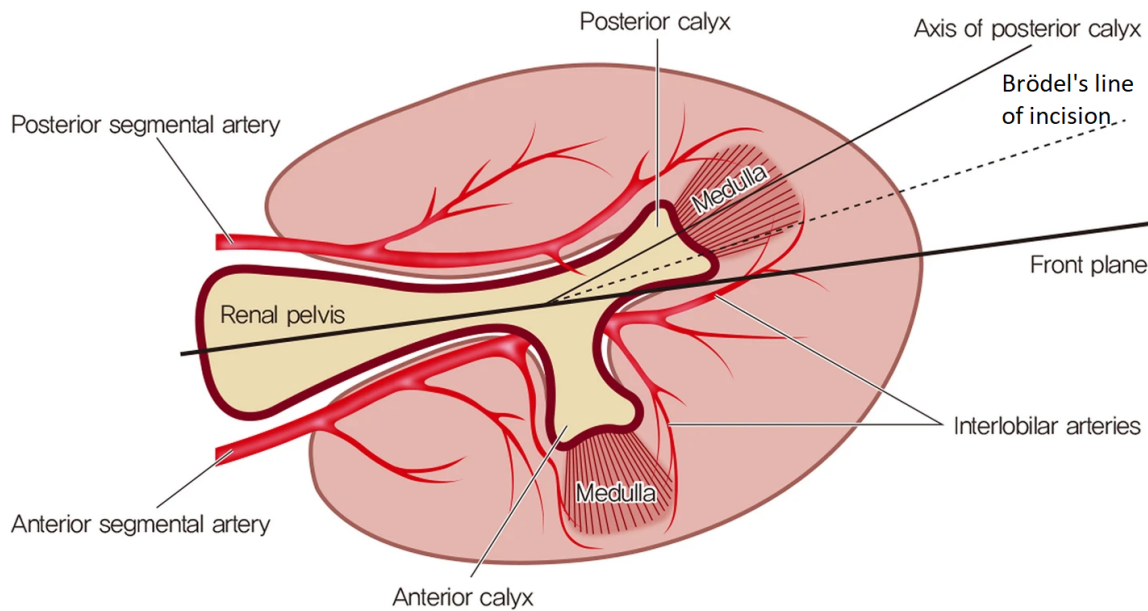
Figure 1.2: Access through a posterior calyx is preferred for lower risk of vascular injury [44]. Image used with the permission of National Center for Biotechnology Information.
.

Techniques of US-Guided Needle Insertion

US-guided PCA is often performed using a curvilinear ultrasound probe and an 18 gauge needle. During scanning, if the kidney is partially obscured by acoustic shadowing from the ribs, a 30-45 degree rotation can be applied to align the probe to the ribs [19]. Needle insertion can begin once a clear path to the target in the posterior calyx is planned on a longitudinal US view of the kidney [19]. During insertion, the goal is to maintain alignment between the needle and the US beam (needle-beam alignment), in order to visualize the needle in its entirety

(Figure 1.3). If misalignment happens, needle advancement should be stopped, and the US probe should be used to identify and redirect the needle [19]. Successful access is verified on observation or aspiration of urine after removing the stylet [19]. A needle guide would help with needle-beam alignment at the expense of the flexibility of the accessing angle [19].
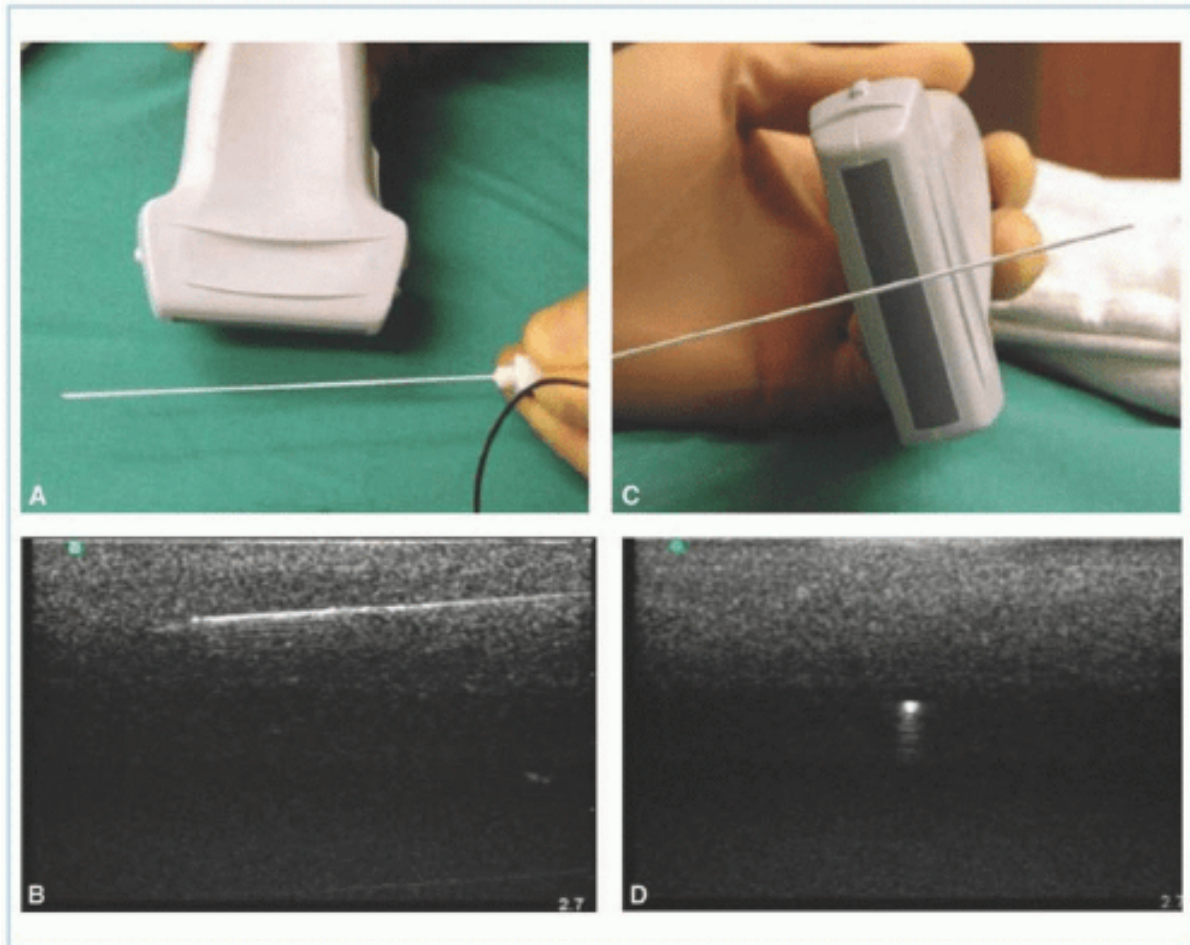
Figure 1.3: In-plane alignment technique (left), needle and US beam are in the same plane. Out-of-plane technique (right), needle is perpendicular to the plane of US beam ([94]. Image used with the permission of Wolters Kluwer Health Inc.

.

Access Related Complications

Hemorrhage is the most common complication of PCA, however, minor hemorrhage during PCA typically does not require intervention. Nevertheless, major hemorrhage happens to 1%-

15% of the patients, requiring blood transfusion [39][74][105]. In addition to renal hemorrhage, inadvertent needle puncture can cause complications in other organs and structures adjacent to the kidneys including thoracic injuries (4%-16%), and visceral organ injuries such as colon injuries (<1%) [39]. Liver and spleen injuries are very rare in the absence of anatomic abnormalities [39][92].

1.1.4   PCA Training Status Quo

In North America, PCA is often performed by interventional radiologists as a staged procedure before planned PCNL [46]. Recent studies have suggested that urologists can obtain PCA safely and effectively, transforming PCNL into a single-stage procedure, which eliminates the need to transfer patients between different departments [23][93]. In addition, having the ability to independently obtain the access provides better flexibility for the urologists, when selecting the optimum tract or making a secondary tract [46][53]. An American survey revealed that urologist-obtained PCA is associated with a higher stone-free rate (86% vs 61%) and lower number of complications (5 vs 15), in comparison with radiologist-obtained PCA. However, only 11% of urologists obtain access themselves, mainly due to the lack of training [101]. Despite previously reported benefits of urologist-obtained PCA, only 37.5% of Canadian residents train at centres where urologists obtain their own PCA, independent of radiologists [72].

At present, US-guided PCA is taught through the traditional apprenticeship approach, where trainees would perform this procedure on patients under the supervision of senior physicians, until the trainee is considered proficient to operate independently. Therefore, factors such as concerns for patient safety, and restricted training hours, limits the trainees' opportunity to gain experience with this procedure [76]. Moreover, achieving competency in PCA is challenging due to the steep learning curve. Two recent studies evaluated the learning curve for US-guided PCNL and reported that it would take 60 cases for novice trainees to gain surgical competency and 120 cases to achieve excellence [85][104]. For experienced surgeons, 20 cases are sufficient for the transition from FL-guided to US-guided PCNL [96]. Furthermore,

competency evaluation is usually conducted by the supervising physician, using checklists or in-training evaluation reports, which suffer from subjectivity [59][64].

1.1.5 Challenges and potential solutions

In summary, US-guided PCA is a challenging procedure associated with a steep learning curve. To achieve competency in US-guided PCA, a trainee should master technical skills, including a good understanding of renal anatomy, the ability to obtain and interpret US images, and proper skills to maintain needle-beam alignment during access [19]. However, the traditional training approach is not sufficient to meet the training demands except at some high-volume centres [46]. Beiko et al. [19] suggested the training be split into two different skill sets, diagnostic renal imaging, and needle control, for a more structured learning approach. More specifically, the authors advised trainees to practice renal US imaging on patients or abdominal phantoms whenever an opportunity arose, to shorten the learning curve [19]. Likewise, training simulators for percutaneous needle access can be a potential solution to the training demand for mastering needle control. To further improve the accessibility, simulated US could be used to eliminate the need to access US machines, providing flexibility in training time and location. In addition, training simulators could provide objective feedback to trainees, decreasing the demands for supervision by senior physicians.

1.2 Simulation-based Medical Education

Training simulators were first used in high-risk professions such as aviation and aerospace, where mistakes can be fatal [73]. Similarly, during a medical procedure, the smallest error could have dire consequences. Medical training simulators provide a stress-free and harm-free environment for health professionals to acquire knowledge and surgical skills through deliberate practice [82]. More importantly, simulation-based training can minimize risks as the trainees begin to operate on patients [5]. While simulators are no substitute for clinical training

in the operating room (OR), they can nevertheless help to shorten the learning curve [3][54]. A number of laparoscopic and endoscopic training simulators have demonstrated the transfer of skill from a virtual environment to the operating room [80]. Therefore, simulation-based training is now considered an essential adjunct to the traditional apprenticeship training, and it has been successfully adopted by some centres [4][81]. However, a recent survey from the United Kingdom indicated the lack of simulation-based training for many standard urology procedures including PCA, possibly due to the high cost of the existing simulators [64].

1.2.1 Simulator Fidelity

Existing medical training simulators can be categorized into low-fidelity (LF) and high-fidelity (HF) trainers based on their physical resemblance to the surgical procedure. Commonly used LF simulators including intravenous injection trainers, silicone pads for suture practice, box trainers for laparoscopic and endoscopic procedures, etc. A LF simulator typically provides training on a specific task that is designed to improve manual dexterity, hand-eye coordination, or tissue handling [78]. Even though these simulators have limited functionality, they are usually highly portable, easy to set up, and low maintenance [78]. Above all, they are very effective for novice trainees to acquire the basic surgical techniques at the initial stage of training. [78].

HF simulators are mostly computer-based applications, working in conjunction with hardware such as surgical tool emulators, haptic devices, tracking systems, phantoms, or manikins, for complex procedure simulation. One common approach to creating a training scenario that resembles the actual surgical procedure is to replicate it digitally, in a virtual reality (VR) environment. The other option is to artificially enhance the physical world with additional information in the form of a digital overlay, in other words, augmented reality (AR) [98]. In the field of urology, AR/VR simulators are widely used for endoscopic and laparoscopic training [31]. A significant advantage of AR/VR simulators is their ability to record training data, which could be used for progress monitoring or providing objective performance feedback. Compared to

the other types of simulators, the AR/VR technology offers the freedom to simulate various clinical scenarios, a range of tasks and difficulty levels, and patient-specific anatomies [64]. On the flip side, the cost of development and maintenance may be much higher. Live animal models are also considered high fidelity as they provide realistic haptic feedback, respiratory movement, and bleeding [4]. However, due to the limited supply, cost, and ethical considerations, live animal models are not suitable for repetitive practice[8].

It is commonly believed that the effectiveness of a simulator improves as its realism increases. Yet, this is only partially true. Beyond a certain level, the simulator performance reaches a plateau, regardless of the amount of money and effort invested [52]. A large body of studies has demonstrated that HF simulators are not necessarily more effective than LF, evidently suggesting that learning outcomes of training simulators are independent of their physical fidelity [20][55][61][78]. Instead, more attention should be paid to the psychological process during a surgical procedure [57][21]. Simulator design should follow a minimalist approach to direct the focus of the user to the critical tasks after establishing the objectives of training and intended trainee group [21][61]. Any additional non-essential information could potentially cause distraction or cognitive overload [57][21]. In addition, other aspects, including the accessibility, versatility, reproducibility, and maintenance requirements, should also be considered during the design process [20].

1.2.2 Review of Existing Training Simulators for PCA

Existing training simulators can be grouped into the following categories: live animal models, biological or non-biological bench models, and VR/AR-based simulators [64].

Live Animal

Two studies have reported the use of anesthetized live porcine models for PCA training, mainly because of the similarity of the pig and human renal anatomy [41][58]. In addition, such models provide tactile feedback, respiratory movement, and bleeding that is superior to other

types of training simulators [58]. However, training on live animals requires ethics approval, and veterinary support, which also increases the training cost [58]. Therefore, the use of live porcine models for training is limited. Mishra et al. [58] concluded that live porcine models are more suitable for skill assessment.

Biological Bench Models

Bench models made of ex-vivo porcine or bovine kidneys were the most common type of PCA trainers from the 2000s to early 2010s [64]. The dissected kidneys were wrapped within various types of materials including foam [22], sponge [1], silicone [87], chicken carcass [32][35][100], as well as a combination of porcine skin flap [37], subcutaneous fascia and muscle [40][107], and ribs (figure 1.4) [26][88][109]. These trainers are generally cheap and easy to make. Furthermore, artificial stones can be manually placed into the renal pelvis for PCNL training. Similar to the live animal model, biological bench models are designed to work with image-guidance equipment and thus require wet lab access. While all except for one of these trainers can be used for FL-guided PCA, four of them are not US compatible [22][1][32][100]. In addition, each biological bench model can be used only for a limited number of times. All of these factors limit the accessibility, versatility, and reproducibility of these biological bench models.
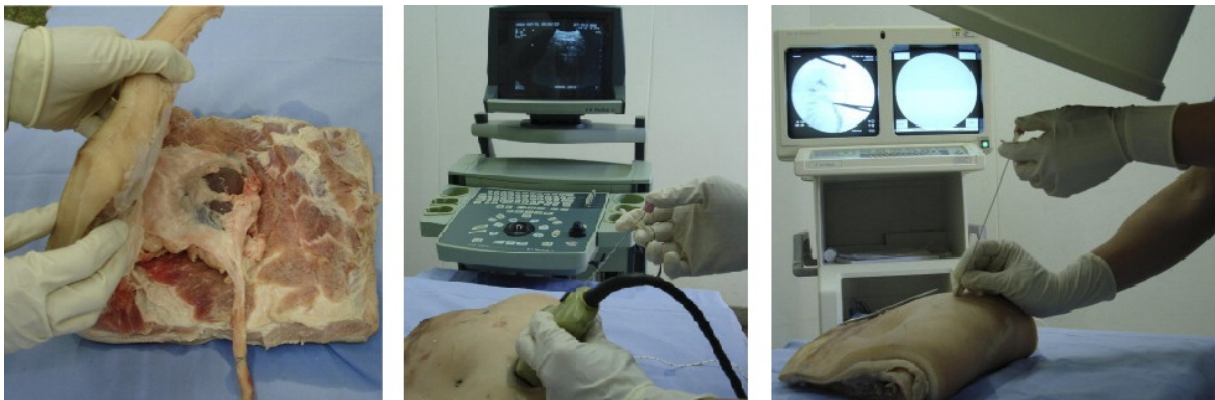
Figure 1.4: An example of ex-vivo porcine model for US/FL-guided PCA training [107]. Image used with the permission of Elsevier.

.

Non-Biological Bench Models

Since the mid 2010s, there has been an increase in research involving non-biological bench models, ranging from the low fidelity vegetable [83] or sponge [91] to anatomically correct silicone [106] or hydrogel [30] kidney models, to highly detailed three-dimensional (3D) printed silicone models based on patient CT scans [14][95][103]. All of the above models were design for FL-guided PCA with no US compatibility. Only three commercial US compatible bench models exist for full PCNL procedures: the PCNL trainer (Encoris), Perc Trainer (Mediskills), and PCNL trainer LS40 (Samed GmbH Dresden). These synthetic training models require a dry lab setting and access to C-arms or US machines.

To eliminate radiation exposure during FL-guided PCA training sessions, Veneziano et al. developed a 3D printed mini C-arm trainer (SimPORTAL), using two webcams to simulate FL images, and a silicone flank model for needle insertion (figure 1.5) [66][99]. Images obtained from the cameras were filtered and fused together through the "chroma-key" technique [99]. This low cost replication of a C-arm provides a radiation-free training environment and dramatically improves the accessibility.

In summary, the artificial bench models are more accurate at replicating human anatomy, and more durable than the biological bench models for repetitive practice. However, their tactile feedback is inferior to that provided by biological tissues. One common drawback of these bench models is the lack of performance feedback to trainees. Hence the presence of an expert may be required to provide guidance [24].

VR/AR-based Simulators

The PERC Mentor (Simbionix) was the first VR simulator for FL-guided PCA, which has been thoroughly validated for training and assessment purposes. This simulator features several training scenarios of increasing complexity which were created in a virtual surgical environment, a virtual C-arm controlled by the touch screen or a foot pedal, a sensorized needle for location tracking, a torso mannequin that mimics various human tissues embedded with
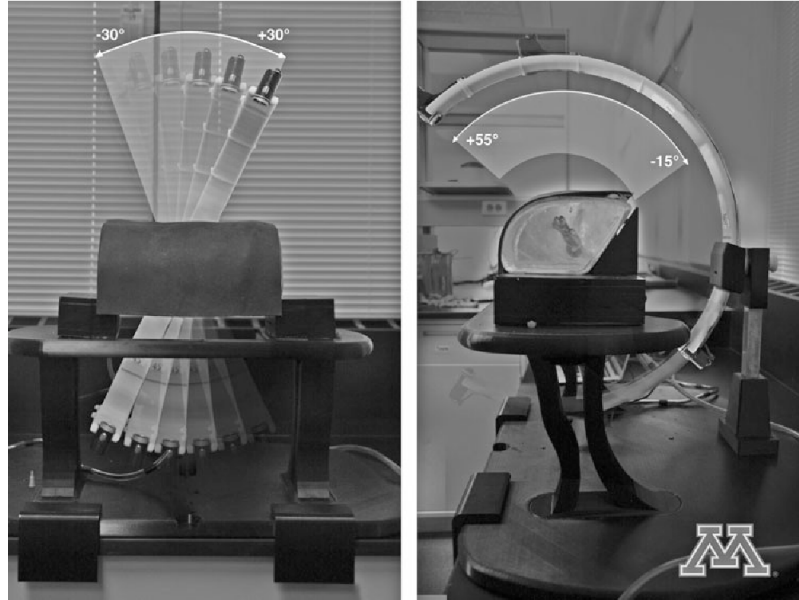
Figure 1.5: SimPORTAL-A mini C-arm simulator and a silicon flank model for radiation free PCA training [99]. Image used with the permission of Mary Ann Liebert Inc.

.

palpable ribs, the visualization of the virtual anatomy with respiratory movement, a virtual assistance providing warnings and directions, and performance reports of recorded training parameters such as operation time, FL time, number of attempts, rib collisions, injuries to adjacent organs, etc. [63]. A number of studies have reported its face [45][60][81], content [45][58][60][81], construct [28][45][60][81], and predictive validities [54][60], as well as skill acquisition of trainees [28][56][69][108]. Furthermore, two studies reported using the PERC Mentor for PCA assessment [63][65]. However, the PERC Mentor hasn't been widely adopted by training centres mainly due to the high cost ($100,000)[64].

In 2019, Tai et al. [90] published a study of a novel AR-based simulation platform —SimPCNL for FL-guided PCA training. SimPCNL consists of a PC, two PHANTOM Omni devices that provide realistic tactile sensation, and a Microsoft Hololens, which provides an AR view of the surgical scene [90]. The combination of visual and haptic simulation effectively replaces the traditional training phantoms. More importantly, the force feedback from the haptic devices is used for physics-based tissue mesh deformation in real-time [90]. These force and velocity

data are also recorded as valuable evaluation parameters [90]. In this study, the authors successfully demonstrated the face, content, and construct validities of this simulator [90]. Criterion validity was also established through a comparison with the PERC Mentor (figure 1.6)[90]. Even though the cost of the Hololens and the PHANTOM Omnis is higher compared to the bench models, this simulator is much cheaper and more portable than the PERC Mentor .
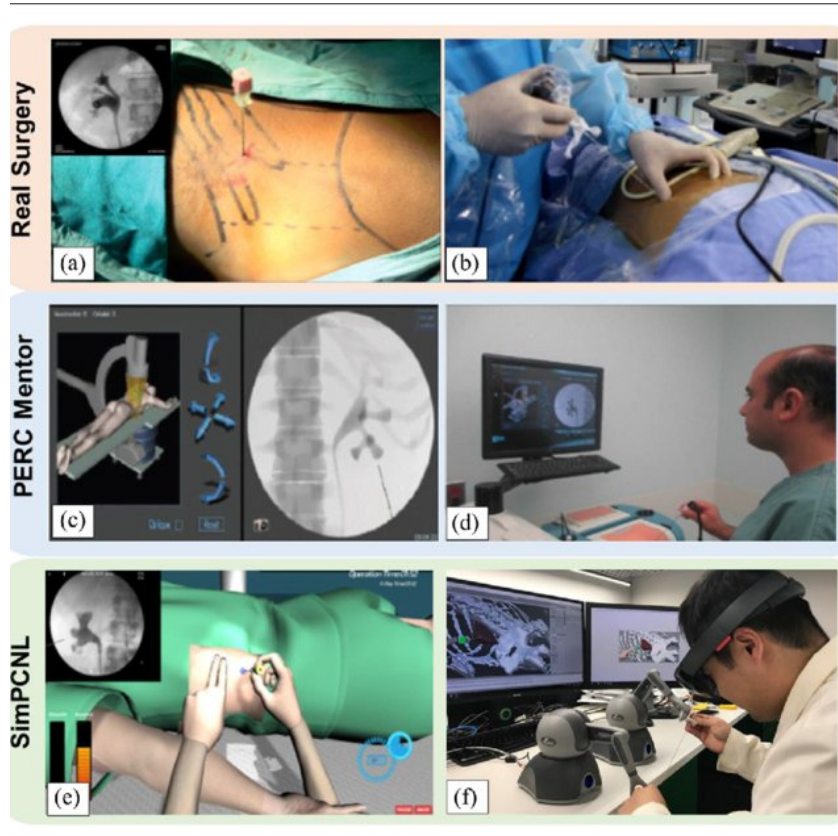
Figure 1.6: Comparison between real surgery, PERC Mentor, and SimPCNL. The left column displays the surgical interface. The right column displays the operation scene [90]. Image used with the permission of SAGE.

.

In conclusion, AR/VR training simulators can simulate various training scenarios, record objective performance parameters for skill assessment, and provide a radiation-free environment for repetitive, deliberate practice. Yet, both of these simulators are designed for FL-guided PCA. No AR/VR training simulator was reported for US-guided PCA.

1.2.3   Challenges and possible solutions

In a review study of 109 articles of simulation in medical education, Issenberg et al. [9] reported the top simulation features lead to effective learning are feedback (47%), repetitive practice (39%), curriculum integration (25%), and range of difficulty levels (14%). AR/VR training simulators have a clear advantage over bench models and live animal models in providing these features. The existing AR/VR simulators are validated but underutilized due to their high cost, highlighting the need for a low-cost simulator for US-guided PCA.

Visualization

Two types of AR/VR visualization devices are monoscopic devices, including cellphones, tablets, monitors etc, and stereoscopic head-mounted displays (HMD) such as the hololens, Vive (HTC), Google Cardboard, etc. The high-end HMDs are often equipped with multiple sensors and cameras for tracking the user's poses relative to the surrounding environment. Google Cardboard or similar passive devices can be used with cellphones to provide a stereo view. The simpler mobile devices merely serve as a display (VR) or capture video of the real world using a single camera (AR). Even though stereoscopic devices enhance depth perception, selection of an AR/VR device should be made according to the surgical scenario.

During an actual needle access procedure, the physician would be standing at a fixed location, operating at elbow height. His/her head motion would be limited, switching focus between the operating hands and the US display. Thus the viewpoint can be fixed once the procedure starts during training. The advanced HMDs provide no additional benefit over a simple mobile device for operator tracking.

US simulation

Since there is limited availability of US machines, US simulation would significantly improve the accessibility of a training simulator. There are two different approaches to simulate US images: real-time simulation based on mesh models [11], or manipulation of pre-recorded US

volume, each having its own advantages and disadvantages.

The pre-recorded US image approach would be more realistic than the use of simulated images, but it requires scanning of the real-patient for each training case. Additionally, the US effect of a needle needs to be added to the volume in real-time, which requires more programming effort, since the AR/VR development platform (Unity) has very limited capability for processing medical images. However, it is feasible to expand Unity's functionality via native plugins in order to achieve the desired result. However, this simulation approach heavily relies on the processing power of the mobile device.

On the other hand, the PLUS toolkit [11] can be used to simulate US images based on mesh models of the renal system and the needle. The acoustic properties of different tissues and material can be carefully customized for optimum results. This process can be performed on a PC/server to reduce the workload on a mobile device. Transmission between the PC/Server and the mobile device can be established via a simple communication plugin.

Tracking

Optical tracking and electromagnetic tracking (EMT) are the most commonly used systems for surgical navigation, with both systems providing sub-millimeter tracking accuracy. However, the optical systems require a direct and continuous line of sight between the sensor and the camera, and the EMT systems are prone to interference from metallic objects and electromagnetic fields [50]. Vuforia is a proprietary image processing software development kit (SDK) that uses feature detection algorithms to register and track image markers or 3D objects. Setting up the system only requires registering a unique marker to the Vuforia database, then attached it to an object which needs to be tracked. A camera is also required to capture the images, which is available on almost all mobile devices. The tracking accuracy of Vuforia varies, depending on the quality, size of the image, the camera resolution, and the lighting condition. With the new generation of mobile devices featuring depth-sensing cameras, the image tracking accuracy would be greatly improved.

Phantom

Haptic devices such as the PHANTOM Omni provide superior haptic feedback compared to that provided by simple artificial phantoms. Although it costs over $1000 and the range of motion is limited. Poniatowski et al. [71] studied the needle insertion forces for PCA on a human cadaver. While the peak of the force-depth representing skin puncture is evident, the peak representing renal collecting system puncture is non-uniform and indistinguishable at times. Therefore, confirmation of perforation of the renal collecting system should not be relied on using haptic feedback.

A wide variety of hydrogel or silicone materials is available for fabricating tissue mimicking phantoms. The hydrogel-based materials are often used to make US compatible phantoms, because their acoustic property is similar to that of human soft tissue [17]. However, some of these hydrogel materials degrade rapidly due to microbial invasion and dehydration [67]. Poly(vinyl alcohol) cryogel, PVA-C, is a magnetic resonance imaging (MRI) and US compatible material that can be preserved for several months [89]. But it cannot sustain repetitive needle puncture. While silicone materials are more durable for practicing needle insertions, their acoustic properties do not match those of human soft tissue. Maggi et al. [51] reported that the attenuation of silicone could be modified with additives if US compatibility is desired.

1.3   Objective

The objective of this thesis work was to develop a low-cost and accessible AR training simulator for US-guided PCA, utilizing personal mobile device and off-the-shelf components, to provide extra training opportunities to novice trainees, in addition to the traditional apprenticeship approach.

1.4   Thesis Outline

In response to the limitations of current systems outlined above, Chapter 2 of this thesis describes the development of a novel AR training simulator for US-guided PCA as well as the validation steps and results. Chapter 3 then discusses the advantages and limitation of the current work and proposed directions for future research.

Chapter 2

Development and validation of an augmented reality simulator for ultrasound-guided percutaneous renal access

This chapter is adapted from the following manuscript:

- Yanyu Mu, David Hocking, Zhan Tao Wang, Gregory J. Garvin, Roy Eagleson, and Terry M. Peters. "Augmented reality simulator for ultrasound-guided percutaneous renal access." *International Journal of Computer Assisted Radiology and Surgery,* 15(5):749–757, 2020.

2.1   Introduction

As reviewed previously, ultrasound (US)-guided percutaneous renal access (PCA) is gaining popularity over fluoroscopy (FL)-guided PCA for better procedure outcomes and reduced radiation in minimally invasive treatment of renal disease. However, the current apprenticeship

training cannot meet the growing training demand. As a supplement, simulator training can provide additional learning opportunities to novice trainees. Several augmented reality (AR)/ virtual reality (VR) simulators for FL-guided PCA were reviewed in chapter 1. One of the main reasons that simulators are underutilized in training is their high cost. Therefore, we identify the need for a cost-effective, versatile and easily accessible simulator for US-guided PCA training.

In this chapter, we propose the development of a novel AR simulator, emphasizing the use of off-the-shelf components and incorporating a simple and easily made physical phantom for US-guided PCA, and evaluated its validity and efficacy as a teaching tool. The major contributions of our simulator are as follows:

1. The simulator was designed to exploit the popularity of modern portable devices and personal computers, which allows the trainees to use their personal devices for visualization and computation. This approach significantly reduces the cost and improves the accessibility of our simulator.

2. Through computer vision-based tracking of a silicone phantom, an US probe emulator, and a needle via a mobile device camera, we are able to simulate a virtual PCA procedure for the user to have a realistic training experience under AR without the need of any external tracking device. This implementation further reduces the cost.

3. Virtual anatomy models with different patient pathologies can be imported into our simulator as training cases, making it customizable for educators to create a variety of clinical scenarios ranging from common to extremely rare.

2.2   Material and methods

2.2.1   Phantom

The phantom consists of two layers of silicone, a 3mm deep skin mimicking layer on top of an 8.5cm deep soft tissue-mimicking layer. The skin mimicking layer was fabricated using a two-part silicone (Ecoflex 0010, Smooth- On inc., USA) with a Shore hardness of 00-10. Ecoflex® part A and part B were mixed with a 1:1 ratio by weight and cured at room temperature overnight. The cured surface was powdered with talc to create a dry and smooth surface for smooth movement of the US probe emulator. To achieve the softness of human soft tissue, a silicone tactile mutator Slacker® (Smooth-On inc., Macungie, PA, USA), Ecoflex® part A, and Ecoflex® part B were mixed at 2:1:1 ratio by weight. Although Slacker® provides many benefits such as increasing the softness, rebound, and self-healing properties of silicone [67], it also increases the tackiness which leads to greater friction during needle insertions. Consequently, we observed a small amount of silicone adhered to the needle shaft after each needle withdrawal. Glass microspheres have been used primarily as a filler material in the industry due to its low density. We introduced glass microspheres into the silicone mixture at a 4% weight ratio, which resulted in smoother needle insertion, and no silicone material adhesion to the needle shaft. We speculate that the ball-bearing property of glass microspheres effectively decreased the friction on the needle shaft, while maintaining the overall softness, rebound, and self-healing properties of the modified silicone.

2.2.2   Hardware

Initial Design

The initial design utilized Google Cardboard combining with a cellphone to provide better depth perception through immersive stereoscopic visualization. However splitting the cellphone display for stereoscopic view dramatically restricted the field of view (FOV). Moreover,

the generated stereoview was provided at the cost of a lower resolution, which was not suitable for inspecting details of the virtual renal anatomy at the operating distance. Lastly, the latency introduced by the software, that caused a perceptible lag between the time the US transducer or needle was moved, and the appearance of this motion on the display, induced motion sickness and eye fatigue while wearing a HMD [33]. Hence, a simple monoscopic mobile device was considered a more efficient and cost-effective option for visualization purposes.

Final Version

During the performance of a PCA, the physicians need to check their hand movement or the US machine display intermittently to confirm probe and needle position with reference to the US image. These head movements complicate the procedure, making it more challenging for novice trainees to master the basic techniques such as in-plane needle alignment. We eliminated the need for these head motions by combining the US image stream with the camera feed of the surgical site on the same tablet screen, therefore, providing a more intuitive user experience. The tablet screen was split into two sections: the top for the US image stream and the bottom for camera feed (Figure 2.1 Left). The tablet utilized in this project is a Samsung s5e (Samsung Electronics Co., LTD., Suwon, South Korea) with a 13-megapixel rear camera.

To track the poses of the US probe emulator, needle, and silicone phantom in real-time, unique image markers must be attached to each component securely. For this purpose, we designed the attachments for the needle and silicone phantom (Figure 2.1 Right) with Space-Claim 19.1 (SpaceClaim Corp., Concord MA, USA). The stereolithography (.stl) file of an Ultrasonix C5- 2/60 curvilinear US probe model was downloaded from Plus toolkit printable three-dimensional (3D) models catalog (Perk Lab, Queen's University, Kingston, ON, Canada), then modified to incorporate an image marker. All components were then 3D printed using the Ultimaker 3 (Ultimaker B.V., Geldermalsen, Netherlands).
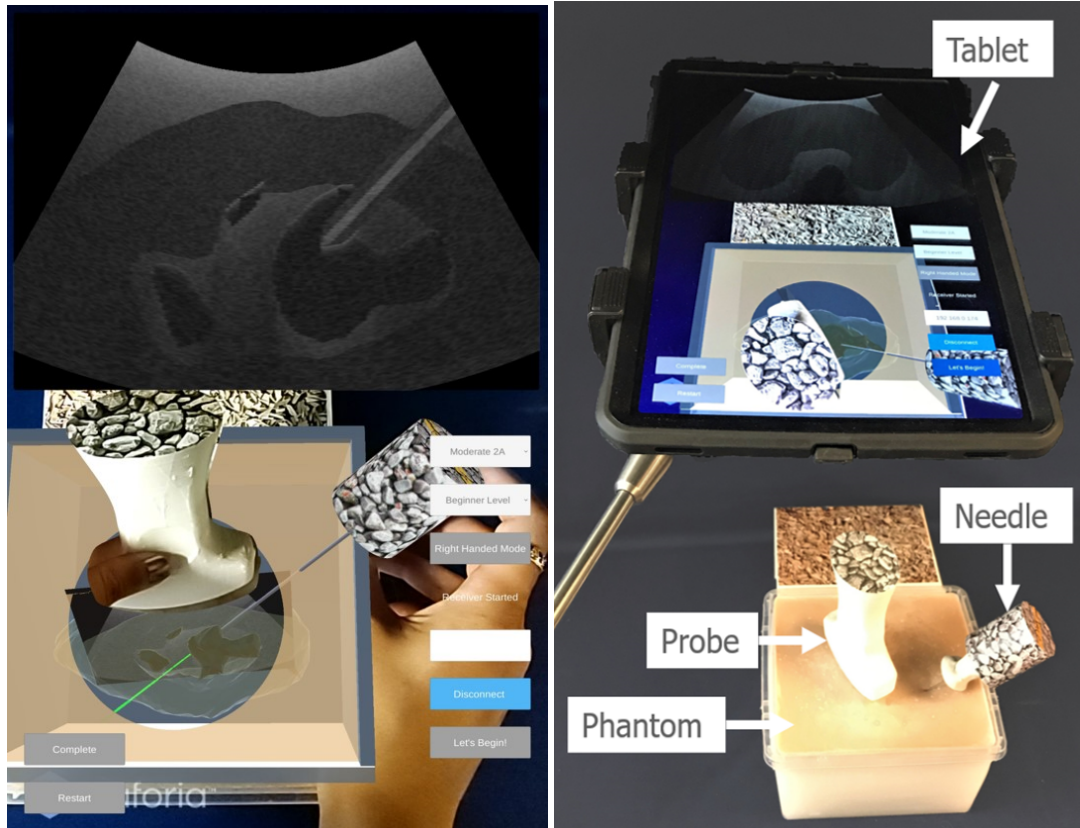
Figure 2.1: AR visualization and system hardware. (Left) The top section displays real-time 2D US simulation and the bottom section displays the 3D AR scene of PCA with full AR assistance. (Right) The hardware setup including a mounted tablet, a 3D printed probe emulator, a needle, and a silicone phantom. Image used with the permission of Springer Nature.

2.2.3 Software

Segmentation and three-dimensional (3D) model construction

The 3D kidney models were generated retrospectively from diagnostic nephrostomy computed tomography (CT) studies stored in a PACS database. Recent Nephrostomy tube insertion cases were reviewed by one of the interventional radiologists along with preceding CT studies. Five cases were selected based on hydronephrosis grade including one mild, two moderate, and two severe cases. Hydronephrosis is the swelling of a kidney caused by a blockage that doesn't allow proper urine drainage. The segmentation of the renal parenchyma and collecting system was performed by the same radiologist using TeraRecon Aquarius iNtuition ver.4.4.13.P2 (TeraRecon Inc., Foster City, CA, USA). The parapelvic fat, renal masses, and cysts were excluded from the segmentation and the proximal ureter was included only to the level of the lower pole of the kidney. The gross contour of the kidney was manually interpolated across these structures. Finally, the segmented volumes were converted to meshes and exported as .stl files.

Vuforia tracking

Infrared optical, electromagnetic, and GPS tracking systems are well-established for real-time tracking of surgical instruments in surgical navigation for their high accuracy. However, due to their complex setup and high cost, training simulators employing these tracking systems are not widely adopted in medical schools. As AR applications increase in popularity, computer vision-based camera tracking has become an active research area. Vuforia software development kit (SDK) (PTC Inc., USA) is licensed software that uses its proprietary computer vision-based image recognition algorithm to track 2D images or 3D objects in real-time by detecting sharp corners and edges from camera images. Based on detected features, the position and orientation of the marker in the virtual space are computed using affine transformation. Three unique, non-repetitive Vuforia markers were used to estimate the locations and orientations of

the needle, the US probe emulator, and the silicone phantom. To use Vuforia marker, a digital copy of the image needs to be uploaded to Vuforia server for feature detection (Figure 2.2). The digital markers were cropped and adjusted to ensure good visibility of texture details under the camera, which improved the performance of feature recognition and the robustness of object tracking. The physical dimensions of the printed markers were measured using a caliper then the processed marker data were imported into Unity (Unity Technologies, USA) at 1:1 scaling ratio. 3D virtual models of the needle, the US probe emulator and the silicone phantom were registered to the markers in the Unity. Once a marker was identified, the corresponding virtual object appears on the screen based on the pose of the marker. The dimensions of virtual objects are the same as the physical models. The data stream, referred to as the tracker stream in this chapter, containing positions and orientations of these virtual objects was packaged in Unity and then used for US simulation. The tracking precision of the needle marker was tested on a 20×20 cm grid placed 30 cm away from the tablet camera at 45° angle to simulate the tracking area during training. 225 tracking positions were recorded at various needle poses angled within 30° from the grid surface normal. The tracking error is consistently low over the entire tracking area with a mean and max error of 1.7 mm and 3.5 mm respectively.
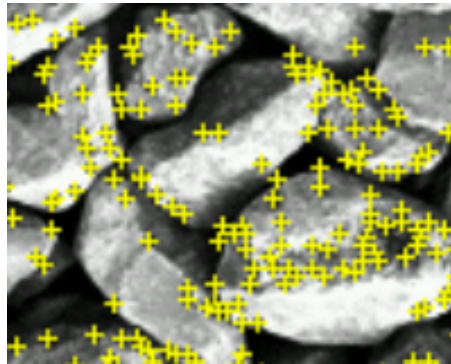
Figure 2.2: An simplified result of Vuforia feature detection.
.

Simulation workflow

An overall deployment diagram is shown below in Figure 2.3. In this project, we used the previously validated public software library for US imaging research (PLUS) for real-time US image simulation [11]. PLUS accepts the tracker stream and the mesh models of the kidney and the needle as inputs to compute individual US scanline based on the pose of the probe. Acoustic properties of each mesh model, including attenuation, absorption, and reflection, were modified in the configuration file (Appendix A.) to achieve the most realistic simulation effect. However, this algorithm does not simulate characteristics of real ultrasound images such as speckle and reverberation. It is important to set up a proper environment for the kidney model in the configuration file to simulate the US effect of kidney In Vivo. Therefore, layers of material were configured such as air, a working volume of gel, the kidney shell, and the collecting system. Similarly, a needle would appear as a thin line on simulated US. Adding a concentric tube over the needle model created a halo effect which is more realistic. To optimize the processing performance of the tablet, PLUS was configured to run on a separate PC.

Data transfer between the tablet and the PC was achieved through a communication plug-in built for Unity, which is a modified version of open image-guided therapy link (OpenIGTLink). Since the original OpenIGTLink was written in C/C++, while our Unity application was written in C#, marshaling methods (Appendix B.) were used to write the Unity implementation to transfer data between managed and unmanaged codes. The modified code (Appendix C. & D.) was compiled to a dynamic-link library (DLL) in Visual Studio. However, to create plug-in that works on Android devices, an extra step is required to cross-platform compile our code into shared object library (.SO) using Android Studio. Once the communication is established between the tablet and the PC, the tracker stream is transmitted to PLUS for US simulation, and the simulated images are sent back to our Unity application in raw data format.
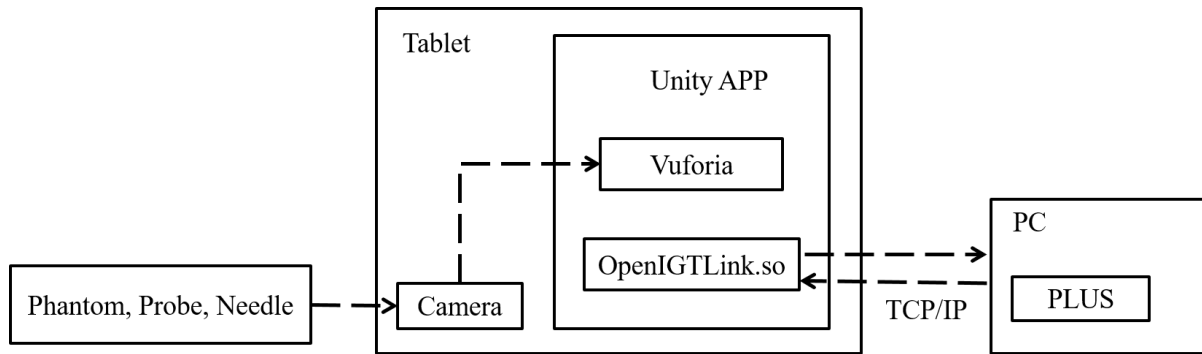
Figure 2.3: Simulation workflow diagram. Image used with the permission of Springer Nature.

AR visualization

To simulate the PCA training environment, we imported models of the 3D kidney, the US probe, and the virtual needle into a Unity scene. Nevertheless, when rendering an AR scene, virtual objects were always drawn on top of real objects, which caused the kidney to appear floating above the silicone phantom. To correct this depth perception problem, we placed the virtual kidney model inside a virtual box, that was manually registered to the phantom container. The illusion of a hollow box can be created by applying depth mask outside of the hollow area (colored in blue), to lower the render queue of the virtual walls (Figure 2.4). A virtual skin layer with a keyhole cutout was placed to help users focus on the region of interest (ROI) while providing additional depth cues. The virtual skin layer was manually registered to the surface of the phantom using the needle tip. A similar floating rendering effect also affects the US probe. While using the probe, the user's hand could be completely occluded by the virtual probe model, creating a disconnect between the real world and the virtual one. We applied the same depth mask technique to the virtual probe model to lower the render queue of the virtual probe model. As a result, the camera feed of the probe was drawn first, which allows the user to see part of the hand holding the probe.

Three training levels (beginner, intermediate and advanced) were designed for users with different skill levels. In the beginner level, a small US image plane was attached below the probe, which helps the user understand the 2D US image within the context of the 3D kidney
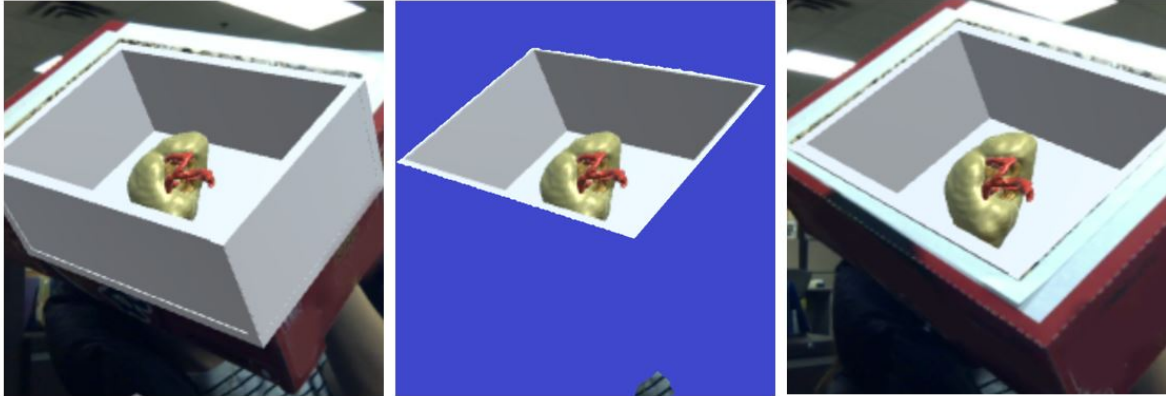
Figure 2.4: Demonstration of depth mask effect. Left: The wall of the hollow white box were visible. The white box appears to be floating on top of the red box from camera feed. Middle: Depth mask was applied to the blue area. Right: The walls of the red box from camera feed was drawn before the virtual white box.

model. In addition, the needle trajectory was also provided to the user, shown as a green projection line attached to the needle tip, serving as a visual aid for in-plane needle alignment (Figure 2.1 Left). Once the user had developed a good understanding of the anatomy and US images, the virtual kidney model was switched off in the intermediate level, while the augmented needle trajectory was still available. Finally, all the virtual aids, including the virtual kidney model, the augmented needle trajectory, and the US image plane below the probe were switched off at the advanced level. The users were expected to complete the task at the advanced level relying solely on the US display.

2.2.4   Simulator Training Procedure

To perform a PCA effectively, a user first inspects the US scans to identify the target inside the virtual kidney (the posterior calyx of the lower pole), under the simulated US guidance. Careful planning should be undertaken to achieve a direct needle access with the shortest path. Once the needle insertion path is planned, the user begins to insert an 18 gauge needle into the phantom, and guide it towards the target. As the needle advances inside the virtual kidney, it is crucial to maintain the in-plane view of the needle in the US image, in order to visualize the needle tip position. Losing track of the needle tip could cause severe complications by
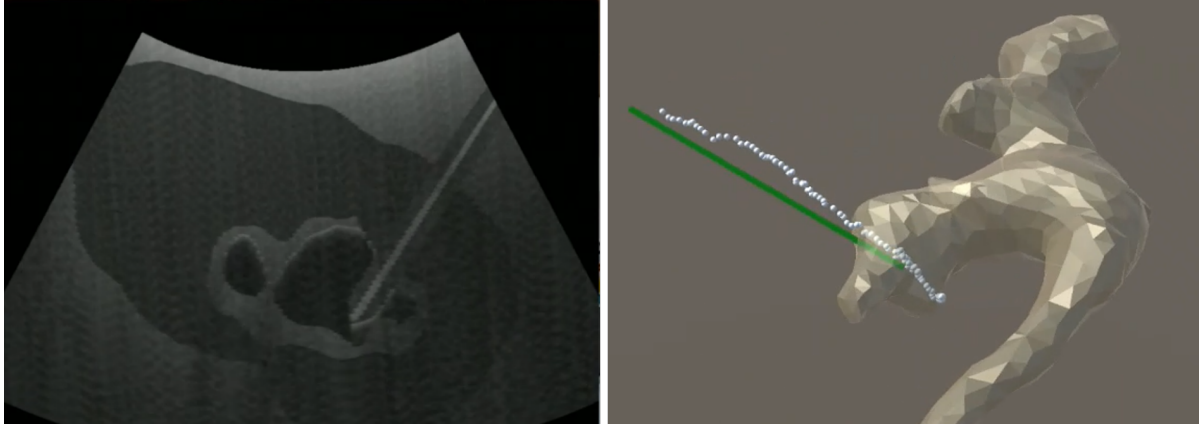
Figure 2.5: Screenshot of the result scene displaying the optimum access trajectory in green line and the user needle trajectory in white dotted line. Image used with the permission of Springer Nature.

inadvertently injuring critical tissue structures. Once the target area is reached, the user presses the 'Complete' button to terminate the simulation and review the needle access trajectory.

For user performance evaluation, a cone-shaped target region was manually registered to each virtual kidney, of which the central line was defined as the optimal needle access trajectory. This cone-shaped target region remains invisible to the users unless the 'Show Hint' button was pressed. The actual needle trajectory was recorded automatically once the needle tip pierces through the skin layer of the silicone phantom at a rate of 10 records per second. After the 'Complete' button is pressed, the application switches to the result scene where users receive intuitive visual feedback of their performance. An overlay of the optimal needle access trajectory (green line), the actual needle trajectory (white dots), and the transparent collecting system model are displayed in the result scene (Figure 2.5).

2.2.5   Evaluation Metrics

The following seven metrics are recorded by the simulator to evaluate user performance.

1. Final distance to target: the distance from the final needle tip position to the optimum target position.

2. Total path length: the total distance that the needle tip traveled in the phantom.

3. Total time: the total time from the moment that the needle tip entered the phantom until 'Complete' button was pressed

4. Overall adaptive distance: the weighted Euclidean distance from the actual needle path to the optimal trajectory (2.1), where N represents the total number of data points, w_i represents the adaptive weight based on the needle insertion depth: $1 - e^{-(depth/0.3)}$, and d represents the Euclidean distance between the needle tip position and the optimal trajectory.

$$WD = \frac{1}{N} \cdot \sum_{i=1}^{N} w_i \cdot d_i \qquad (2.1)$$

5. Needle shaft visualization time: the total time that part of the needle shaft is visible on the US image

6. Needle tip visualization time: the total time that the needle tip is visible on the US image

7. Inside collecting system or not: a binary status indicating whether the final needle tip position is inside the targeted collecting system.

2.3 Validation

To integrate a simulator into the training curriculum, its validity must be proven through an established evaluation process including face, content, construct, concurrent, and predictive validity assessment [10][27][79]. Face validity examines the resemblance between a simulator and the actual procedure, and can be assessed using user survey. Content validity evaluates the educational content of a simulator, and it should be assessed by experts in the field. Construct validity examines whether the simulation performance of a user reflects the actual skill level, which can be assessed by comparing performance of an expert group with an non-expert group. Concurrent validity compares the simulation training effect to an established training method. Finally, predictive validity examines if performance in the simulated environment can

translates to the real world. This can be assessed by correlating simulation performance with the operating room performance. For this study, we focused on the evaluation of face, content, and construct validity.

2.3.1   Experimental Protocol

To validate the effectiveness of our training simulator, we performed a single-centre user study approved by the Health Sciences Review Ethics Board (114409) of Western University. For this study, we enrolled 24 novices and 6 experts on a voluntary basis. The novices consisted of 24 post-graduate medical students with no previous experience in PCA. The experts consisted of urologists and interventional radiologists with over five years of experience in PCA.

For the novices, we started with a five minutes introductory tutorial, which covered the rationale of this study, renal anatomy, targeting, basic US scanning techniques, and AR tracking. When the participants were comfortable with the simulator, the training and testing procedures began. The training and testing procedures were split into three phases including the pre-training testing, training, and post-training testing phases. During the pre- and post-training testing, the simulation was run at the advanced level, which meant no AR assistance was available for the participants. The procedure for pre- and post-training testing were identical. A single PCA procedure was performed by the novices on each of the three kidney models with different grades of hydronephrosis: one severe, one moderate, and one mild case. The evaluation metrics were recorded automatically by the application. In addition, each performance was video recorded and evaluated by two blinded experts using a modified global rating scale (GRS), which includes target identification, US needle tracking, economy of motion, and ability to perform needle access [82]. GRS is a survey tool which has been used to assess clinical competence [36]. During the training phase, the novices had the option to choose the level of AR assistance as they need. One moderate and one mild hydronephrosis cases were used for practicing, which were excluded from the testing cases. Participants were given 15 minutes to practice and ask questions.

Since the experts did not require training, they were given a short introduction of our simulator, followed by five minutes period to familiarize themselves with the system. The PCA procedures were performed by the experts following the same testing protocol for novices. After the session, a standard 5-point Likert scale (1 = strongly disagree and 5 = strongly agree) questionnaire was administered to the experts to assess the face and content validity.

2.3.2 Evaluation Method

First, the face and content validity was evaluated through questionnaires administered to the experts. Second, the construct validity was determined based on the distinguishability of a list of evaluation metrics collected from both novices and experts during needle insertion tasks, where the distinguishability is evaluated using the Mann-Whitney U Test. In addition, we also evaluated the training effectiveness of our simulator based on PCA skill acquisition. The PCA skill acquisition was determined by examining the change in performance of each novice participant based on the parameters collected before and after the training phase, with the paired T-Test being used to analyze the significance of this change. All the statistics were computed using Matlab R2018b.

2.3.3 Results

Face and content validity

The mean scores of face validity statements are detailed in Table 1. In summary, all experts rated the simulator as a 4 or 5 in all categories including the overall realism of the US image, the identification process, and the needle insertion procedure, except for one 3 rating of the needle insertion procedure, achieving an overall average score of 4.39 out of 5 (Table 2.1). In terms of content validity, experts strongly agreed that our simulator is able to teach the basic techniques to perform PCA, such as understanding of the basic anatomy, US interpretation, needle insertion planning, and the in-plane needle alignment with US beam, achieving an overall average

Table 2.1: Mean scores of face and content validity (range 1-5)

Face validity	Expert (n=6)
Realism of the US images	4.39 (4, 5)
Realism of the identification process	4.33 (4, 5)
Realism and usefulness of the needle insertion procedure	4.44 (3, 5)
Content validity	**Expert (n=6)**
Basic renal anatomy	4.80 (4, 5)
Ultrasound images interpretation	4.80 (4, 5)
Safe planning	4.50 (4, 5)
In-plane needle-beam alignment	4.50 (4, 5)
Perform PCA	4.67 (4, 5)
Overall value of the simulator as a training tool	4.16 (4, 5)
Overall value of the simulator as a assessment tool	4.33 (4, 5)
Recommend this simulator to others	4.67 (4, 5)
Use this simulator in your training program	4.33 (4, 5)

score of 4.65 out of 5. Furthermore, experts were extremely satisfied with the overall value of this simulator as a training and assessment tool. They are highly likely to recommend this system to others and use it in their training program.

Construct validity

As depicted in Table 2, experts significantly outperformed novices on 6 of 7 evaluation metrics on the simulator ($p<0.05$). Compared to novices, experts were able to insert the needle closer to the optimum location and optimum trajectory, while achieving a shorter needle path length, a shorter completion time, more accurate needle tip tracking, and a 100 percent success rate to insert the needle inside the collecting system for all trials. However, there were no significant differences in needle shaft visualization time between experts and novices (0.89s vs 0.81s, respectively). We suspect that partially visualizing the needle shaft does not contribute to the overall performance of PCA.

Table 2.2: Construct validity

Construct validity	Novice (n=24)	Expert (n=6)	p-value
Final distance to target (mm)	18.5 ± 8.1	8.7 ± 3	*0.005*
Total path length (mm)	326.1 ± 166.6	175.1 ± 37.7	*0.036*
Total time (s)	36.7 ± 23.5	17.9 ± 5.8	*0.036*
Overall adaptive distance (mm)	15.6 ± 5.7	9.8 ± 3.2	*0.031*
Needle shaft visualization time (%)	78 ± 20	89 ± 9	0.154
Needle tip visualization time (%)	43 ± 19	66 ± 11	*0.006*
Inside collecting system or not (%)	60 ± 43	100	*0.026*

[†]Data in this table are represented in mean value ± standard deviation. Statistical differences were calculated with the Mann-Whitney U test. A p-value<0.05 was considered significant.

Acquisition of US-guided PCA skills

The PCA performances of the novice group was assessed subjectively and objectively both before and after training on our simulator. The objective assessments were based on multiple elements such as operation time, distance, needle visualization, and needle access accuracy, as shown in Table 3. The novice participants demonstrated statistically significant improvements in most categories after training, except for the total time and needle shaft visualization, where the improvements were not significant. The subjective assessments of novice performance were made using a global rating scale (GRS) (range 1 - 5) in four categories, as shown in Table 4. Similar to the objective assessments, the novice participants demonstrated significant improvement in all categories after training.

2.4   Discussion

The introduction of medical simulators has brought promising opportunities for training medical professionals outside of operating room (OR), in a safe and stress-free environment [10]. To overcome the common challenges in terms of cost and accessibility, we developed an affordable and effective training simulator for PCA utilizing portable devices and AR. Using Vuforia, a computer vision-based camera tracking SDK, we are able to track the needle, the US probe

Table 2.3: Novice performance pre-training vs. post-training

Novice (n=24)	Pre-training	Post-training	p-value
Final distance to target (mm)	18.5 ± 8.1	8.7 ± 3.2	*<0.0001*
Total path length (mm)	326.1 ± 166.6	263.9 ± 142.7	*0.04*
Total time (s)	36.7 ± 23.5	30 ± 14.5	0.11
Overall adaptive distance (mm)	15.6 ± 5.7	9 ± 2.5	*<0.0001*
Needle shaft visualization time (%)	78 ± 20	81 ± 13	0.446
Needle tip visualization time (%)	43 ± 19	62 ± 15	*0.0002*
Inside collecting system or not (%)	60 ± 43	94 ± 13	*<0.0001*

[†]Data in this table are represented in mean value ± standard deviation. Statistical differences were calculated with the paired T-test. A p-value<0.05 was considered significant.

Table 2.4: GRS (range 1-5) assessments of novice performance before and after training

Novice (n=24)	Pre-training	Post-training	p-value
Identify Target	3.4 ± 1.2	4.5 ± 0.6	*<0.0001*
US Needle Tracking	2.3 ± 1.2	3.6 ± 1	*<0.0001*
Economy of Motion	3.1 ± 1.3	3.6 ± 1	*0.041*
Ability to Perform Needle Access	2.3 ± 1.2	3.7 ± 1	*<0.0001*

[†]Statistical differences were calculated with Wilcoxon signed-rank test. A p-value<0.05 was considered significant.

emulator, and the silicone phantom through the camera video stream in real-time without the need for any external tracking hardware. As a result, the estimated cost of this simulator can be kept below $100.

In general, the effectiveness of a training simulator is demonstrated through face, content, construct, concurrent, and predictive validities [10][27][79]. Following this convention, we first established face and content validity. The high face and content validity scores demonstrate that our simulator closely resembles an actual US-guided PCA procedure and that the skills required for an successful US-guided PCA using our simulator was similar to the skills required for an actual US-guided PCA. Next, construct validity was clearly indicated by the ability of our simulator to distinguish between novices and experts with a high degree of confidence for 6 out of 7 objective evaluation metrics except for the needle shaft visualization time. In addition, our experiment showed significant improvements in the US-guided PCA skills of the novice participants, which is demonstrated by the consistent increase in both objective evaluation metrics and subjective GRS in post-training testing. Compared with the objective evaluation metrics in pre-training testing, the final distance to the target, the overall adaptive distance, and the needle tip visualization time improved over 40% in post-training testing, which became very close to the experts' performance.

According to the user feedback, all novices agreed that our simulator is easy to use and useful to improve their PCA skills, and they would like to have the option to practice at home using our simulator. The expert group was satisfied with the overall value of this simulator as a training (4.16 out of 5) and assessment (4.33) tool, and they are highly likely to recommend this system to others (4.67) and use it in their training program (4.33), as shown in Table 1. The major area of improvement that the experts have suggested is the occasional tracking instability.

2.5 Conclusions

Our proposed AR training simulator can provide educators with an alternative to allow for additional training opportunities for trainees to acquire basic skills of US-guided PCA in a safe and stress-free environment. The effectiveness of our simulator is demonstrated through face, content, and construct validities. In addition, pre-post testing comparisons showed significant improvements in both the objective and subjective performances of our novice trainees. To further improve the objective evaluation of user performance, our next step is to design an overall scoring system combing the evaluation metrics, which will allow us to assess the concurrent validity of our simulator. In future iterations, with the advancement of mobile computing technology, we would like to incorporate realistic lighting and shadows, as well as tissue deformation characteristics, to further improve the depth perception and realism of our simulator.

Chapter 3

Conclusions and Future Work

3.1 Conclusions

Simulation-based training facilitate the acquisition and refinement of essential skills for percutaneous renal access (PCA) prior to clinical exposure by providing opportunities for deliberate and repetitive practice. The evaluation metrics from our simulator would provide more consistent objective feedback for targeted training of PCA skills and shorten the learning curve during early training, as demonstrated through the substantial performance improvements over a short amount of training time in the novice group. In addition, our simulator offers different levels of augmented reality (AR) assistance, which allows for more customizable, self-directed, and progressive training with increasing difficulty. Aside from skill enhancements, our simulator has a simple setup, which offers the flexibility to train at home. This not only protects patients from unnecessary harm but also provides trainees a stress-free environment for repetitive computer-guided practice. Since the visualization of patient pathology is implemented through virtual modeling, our simulator has the capacity to include a large dataset with a wide variety of clinical scenarios. In addition, the presented ultrasound (US)-guided needle insertions simulation system, utilizing the versatility of AR technology, can be extended to other clinical applications such as spinal needle insertion or central line insertion

The computer vision-based camera tracking for AR has distinct advantages in cost and portability. However, the performance can be sensitive to varying lighting conditions. During the experiment, we noticed mild tracking instability, which could be caused by the internal tracking algorithm and external lighting artifacts such as specular highlights [102]. Therefore, moderately bright and diffused lighting should be provided for the best user experience.

The haptic feedback can be another useful feature to improve the realism of our simulator. Nevertheless, studies have shown that haptic feedback is less reliable compared with visual feedback and may not be necessary for real-time image-guided needle insertion [29]. Hence, our goal is to focus on training the users to perform PCA solely relying on the US images without any AR assistance nor the sensation to confirm calyx puncture. In addition, our general purposed phantom provides us the freedom to simulate patient-specific scenarios without fabricating various physical phantoms, and thus improving the versatility and cost-effectiveness.

3.2   Future Work

As the presented training simulator is a preliminary design, more refinements are needed maximize its benefits. As we mentioned in section 1.1.5, PCA training can be slit into two sections: diagnostic renal imaging and needle control. It would be beneficial to create two corresponding training modules with virtual guidance such as animations and prompts, as well as progress tracking, to provide a structured learning experience and the sense of accomplishment. Additionally, we can apply elements of gamification such as points and leaderboards to increase user engagement. Currently, user performance feedback is provided in the form of direct visualization of the needle path, and data sheets with recorded performance parameters. Thus, to calculate the total point, a marking scheme needs to be developed first to determine the weight of each performance parameter.

Another direction of improvement relies on technology advancement such as depth sensing cameras and the computing power of mobile devices. As mentioned previously, the newer gen-

eration of mobile devices feature depth sensing cameras which can be incorporated into camera tracking algorithms to further improve the tracking accuracy and stability. Improvements in visual fidelity including depth perception and real-time tissue deformation can be implemented, given a powerful mobile chipset.

In this preliminary study, we have successfully established face, content, and construct validity through a user study described in chapter two. The next step is to establish concurrent validity by comparing the performance against a gold standard. Lastly proof of correlation between simulator performance and operating room (OR) performance can be used to demonstrate the predictive validity of this approach.

Bibliography

[1] Mohamed M. Abdallah, Shady M. Salem, Mohamed R. Badreldin, and Ahmed A. Gamaleldin. The use of a biological model for comparing two techniques of fluoroscopy-guided percutaneous puncture: A randomised cross-over study. *Arab journal of urology*, 11(1):79–84, 2013.

[2] Mayank Agarwal, Madhu S. Agrawal, Abhinav Jaiswal, Deepak Kumar, Himanshu Yadav, and Prashant Lavania. Safety and efficacy of ultrasonography as an adjunct to fluoroscopy for renal access in percutaneous nephrolithotomy (pcnl). *BJU International*, 108(8):1346–1349, 2011.

[3] Rajesh Aggarwal, Jonnie Ward, Indran Balasundaram, Parvinderpal Sains, Thanos Athanasiou, and Ara Darzi. Proving the effectiveness of virtual reality simulation for training in laparoscopic surgery. *Annals of Surgery*, 246(5), 2007.

[4] Kamran Ahmed, Muhammed Jawad, Prokar Dasgupta, Ara Darzi, Thanos Athanasiou, and Mohammad Shamim Khan. Assessment and maintenance of competence in urology. *Nature Reviews Urology*, 7(7):403–413, 2010.

[5] Abdulmohsen H. Al-Elq. Simulation-based medical teaching and learning. *Journal of family & community medicine*, 17(1):35–40, 2010.

[6] Nils Alwall. Aspiration biopsy of the kidney1. *Acta Medica Scandinavica*, 143(6):430–435, 1952.

42

[7] Sero Andonian, Cesare M. Scoffone, Michael K. Louie, Andreas J. Gross, Magnus Grabe, Francisco P. J. Daels, Hemendra N. Shah, and on behalf of the Croes Pcnl Study Group Jean J. M. C. H. de la Rosette. Does imaging modality used for percutaneous renal access make a difference? a matched case analysis. *Journal of Endourology*, 27(1):24–28, 2012.

[8] Abdullatif Aydin, Nicholas Raison, Muhammad Shamim Khan, Prokar Dasgupta, and Kamran Ahmed. Simulation-based training and assessment in urological surgery. *Nature Reviews Urology*, 13(9):503–519, 2016.

[9] S. Barry Issenberg, William C. McGaghie, Emil R. Petrusa, David Lee Gordon, and Ross J. Scalese. Features and uses of high-fidelity medical simulations that lead to effective learning: a beme systematic review. *Medical Teacher*, 27(1):10–28, 2005.

[10] E. Z. Barsom, M. Graafland, and M. P. Schijven. Systematic review on the effectiveness of augmented reality applications in medical training. *Surg Endosc*, 30(10):4174–83, 2016.

[11] Laura Bartha, Andras Lasso, Csaba Pinter, Tamas Ungi, Zsuzsanna Keri, and Gabor Fichtinger. Open-source surface mesh-based ultrasound-guided spinal intervention simulator. *International Journal of Computer Assisted Radiology and Surgery*, 8(6):1043–1051, 2013.

[12] Abbas Basiri, Mehrdad Mohammadi Sichani, Seyed Reza Hosseini, Aliakbar Moradi Vadjargah, Nasser Shakhssalim, Amir Hossein Kashi, Mohammadreza Kamranmanesh, and Hamidreza Nasseh. X-ray-free percutaneous nephrolithotomy in supine position with ultrasound guidance. *World Journal of Urology*, 28(2):239–244, 2010.

[13] Scardino PL. Bloom DA, Morgan RJ. Thomas hillier and percutaneous nephrostomy. *Urology*, 33(4):346 – 350, 1989.

[14] Franck Bruyere, Cecile Leroux, Laurent Brunereau, and Patrick Lermusiaux. Rapid prototyping model for percutaneous nephrolithotomy training. *Journal of Endourology*, 22:91+, 2008.

[15] Yiwen Chen, Jianhua Feng, Haifeng Duan, Youwei Yue, Chaofeng Zhang, Tuo Deng, and Guohua Zeng. Percutaneous nephrolithotomy versus open surgery for surgical treatment of patients with staghorn stones: A systematic review and meta-analysis. *PloS one*, 14(1):e0206810–e0206810, 2019.

[16] Thomas Chi, Selma Masic, Jianxing Li, and Manint Usawachintachit. Ultrasound guidance for renal tract access and dilation reduces radiation exposure during percutaneous nephrolithotomy. *Advances in urology*, 2016:3840697–3840697, 2016.

[17] Martin O. Culjat, David Goldenberg, Priyamvada Tewari, and Rahul S. Singh. A review of tissue substitutes for ultrasound imaging. *Ultrasound in Medicine & Biology*, 36(6):861–873, 2010.

[18] Suraj Dahal and Matthew J. Budoff. Low-dose ionizing radiation and cancer risk: not so easy to tell. *Quantitative imaging in medicine and surgery*, 9(12):2023–2026, 2019.

[19] Beiko Darren, Razvi Hassan, Bhojani Naeem, Bjazevic Jennifer, B. Bayne David, T. Tzou David, L. Stoller Marshall, and Chi Thomas. Techniques – ultrasound-guided percutaneous nephrolithotomy: How we do it. *Canadian Urological Association Journal*, 14(3), 2019.

[20] R. Denadai, R. Saad-Hossne, AP Todelo, L. Kirylko, and LR. Souto. Low-fidelity bench models for basic surgical skills training during undergraduate medical education. *Revista do Colégio Brasileiro de Cirurgiões*, 41:137 – 145, 2014.

[21] Frank A. Drews and Jonathan Z. Bakdash. Simulation training in health care. *Reviews of Human Factors and Ergonomics*, 8(1):191–234, 2013.

[22] Pedro P de Sá. Earp. Percutaneous renal surgery: new model for learning and training. *International braz j urol*, 29:151 – 154, 2003.

[23] A.M. El-Assmy, A.A. Shokeir, El-Tabey Mohsen, T., El-Nahas N., A.R., A.M. Shoma, I. Eraky, M.R. El-Kenawy, and H.A. El-Kappany. Renal access by urologist or radiologist for percutaneous nephrolithotomy—is it still an issue? *The Journal of Urology*, 178(3):916 – 920, 2007.

[24] Tamer El-Husseiny and Noor N. P. Buchholz. *Advanced Training of a Practicing Urologist in Stone Disease Management*, pages 855–862. Springer London, London, 2012.

[25] Siavash Falahatkar, Hassan Neiroomand, Ahmad Enshaei, Majid Kazemzadeh, Aliakbar Allahkhah, and Michael Fariad Jalili. Totally ultrasound versus fluoroscopically guided complete supine percutaneous nephrolithotripsy: A first report. *Journal of Endourology*, 24(9):1421–1426, 2010.

[26] Connor M. Forbes, Jonathan Lim, Justin Chan, Ryan F. Paterson, Mantu Gupta, Ben H. Chew, and Kymora Scotland. Introduction of an ex-vivo pig model for teaching percutaneous nephrolithotomy access techniques. *Canadian Urological Association journal = Journal de l'Association des urologues du Canada*, 13(10):355–360, 2019.

[27] A. G. Gallagher, E. M. Ritter, and R. M. Satava. Fundamental principles of validation, and reliability: rigorous science for the assessment of surgical education and training. *Surgical Endoscopy*, 17(10):1525–1529, 2003.

[28] P. Ganpule Arvind, Shashikant Mishra, B. Sabnis Ravindra, Veeramani Muthu, and R. Desai Mahesh. Evaluation and validation of virtual reality (vr) based simulation to develop endourological percutaneous renal access technique for urological trainees. *Journal of Urology*, 181(4S):491–492, 2009.

[29] Oleg Gerovich, Panadda Marayong, and Allison M. Okamura. The effect of visual and haptic feedback on computer-assisted needle insertion. *Computer Aided Surgery*, 9(6):243–249, 2004.

[30] Ahmed Ghazi, Timothy Campbell, Rachel Melnyk, Changyong Feng, Alex Andrusco, Jonathan Stone, and Erdal Erturk. Validation of a full-immersion simulation platform for percutaneous nephrolithotomy using three-dimensional printing technology. *Journal of Endourology*, 31(12):1314–1320, 2017.

[31] Alaric Hamacher, Taeg Keun Whangbo, Su Jin Kim, and Kyung Jin Chung. Virtual reality and simulation for progressive treatments in urology. *International neurourology journal*, 22(3):151–160, 2018.

[32] Lara Hammond, Janet Ketchum, and Bradley F. Schwartz. A new approach to urology training:: A laboratory model for percutaneous nephrolithotomy. *The Journal of Urology*, 172(5, Part 1):1950–1952, 2004.

[33] P. A. Howarth and P. J. Costello. The occurrence of virtual simulation sickness symptoms when an hmd was used as a personal viewing system. *Displays*, 18(2):107–116, 1997.

[34] Matthew Hudnall, Manint Usawachintachit, Ian Metzler, David T. Tzou, Brittany Harrison, Errol Lobo, and Thomas Chi. Ultrasound guidance reduces percutaneous nephrolithotomy cost compared to fluoroscopy. *Urology*, 103:52–58, 2017.

[35] Axel Häcker, Gunnar Wendt-Nordahl, Patrick Honeck, M. S. Michel, Peter Alken, and Thomas Knoll. A biological model to teach percutaneous nephrolithotomy technique with ultrasound- and fluoroscopy-guided access. *Journal of Endourology*, 21(5):545–550, 2007.

[36] Jonathan S. Ilgen, Ma Irene W. Y., Hatala Rose, and Cook David A. A systematic review of validity evidence for checklists versus global rating scales in simulation-based assessment. *Medical Education*, 49(2):161–173, 2015.

[37] F Imkamp, Klot C von, U Nagele, and TR Herrmann. New ex-vivo organ model for percutaneous renal surgery. *International braz j urol*, 37:388 – 394, 2011.

[38] Alexandru Iordache, Catalin Baston, Silviu-Stelian Guler-Margaritis, Emil Angelescu, Vasile Cerempei, Traxer Olivier, and Ioanel Sinescu. Ultrasound for kidney access in percutaneous nephrolithotomy: a contemporary review. *Medical ultrasonography*, 20(4):508–514, 2018.

[39] Jr. Joseph, A. Smith, Howards Stuart, and M. Preminger Glenn. *Hinman's atlas of urologic surgery / [edited by] Joseph A. Smith, Jr., Stuart S. Howards, Glenn M. Preminger ; illustrated by William Winn*. Atlas of urologic surgery. Elsevier/Saunders, Philadelphia, 3rd ed. edition, 2012.

[40] Stephan Jutzi, Florian Imkamp, Markus A. Kuczyk, Ute Walcher, Udo Nagele, and Thomas R. W. Herrmann. New ex vivo organ model for percutaneous renal surgery using a laparoendoscopic training box: the sandwich model. *World Journal of Urology*, 32(3):783–789, 2014.

[41] Panagiotis Kallidonis, Iason Kyriazis, Marinos Vasilas, Vasilis Panagopoulos, Ioannis Georgiopoulos, Mehmet Ozsoy, Jens-Uwe Stolzenburg, Christian Seitz, and Evangelos Liatsikos. Modular training for percutaneous nephrolithotripsy: The safe way to go. *Arab Journal of Urology*, 13(4):270–276, 2015.

[42] Guido M. Kamphuis, Joyce Baard, Matias Westendarp, and Jean J. M. C. H. de la Rosette. Lessons learned from the croes percutaneous nephrolithotomy global study. *World Journal of Urology*, 33(2):223–233, 2015.

[43] Bum Soo Kim. Recent advancement or less invasive treatment of percutaneous nephrolithotomy. *Korean journal of urology*, 56(9):614–623, 2015.

[44] Hee Youn Kim, Kyu Won Lee, and Dong Sup Lee. Critical causes in severe bleeding requiring angioembolization after percutaneous nephrolithotomy. *BMC Urology*, 20(1):22, 2020.

[45] B. E. Knudsen, E. D. Matsumoto, B. H. Chew, B. Johnson, V. Margulis, J. A. Cadeddu, M. S. Pearle, S. E. Pautler, and J. D. Denstedt. A randomized, controlled, prospective study validating the acquisition of percutaneous renal collecting system access skills using a computer based hybrid virtual reality surgical simulator: Phase i. *The Journal of Urology*, 176(5):2173–2178, 2006.

[46] Raymond Ko, Soucy Frédéric, Denstedt John D., and Razvi Hassan. Percutaneous nephrolithotomy made easier: a practical guide, tips and tricks. *BJU International*, 101(5):535–539, 2008.

[47] Mark L. Lessne, Brian Holly, Steven Y. Huang, and Charles Y. Kim. Diagnosis and management of hemorrhagic complications of interventional radiology procedures. *Seminars in interventional radiology*, 32(2):89–97, 2015.

[48] Bannakij Lojanapiwat. The ideal puncture approach for pcnl: Fluoroscopy, ultrasound or endoscopy? *Indian journal of urology : IJU : journal of the Urological Society of India*, 29(3):208–213, 2013.

[49] Randy L. Luciano and Gilbert W. Moeckel. Update on the native kidney biopsy: Core curriculum 2019. *American Journal of Kidney Diseases*, 73(3):404–415, 2019.

[50] Elodie Lugez, Hossein Sadjadi, David R. Pichora, Randy E. Ellis, Selim G. Akl, and Gabor Fichtinger. Electromagnetic tracking in surgical and interventional environments: usability study. *International Journal of Computer Assisted Radiology and Surgery*, 10(3):253–262, 2015.

[51] L. E. Maggi, M. A. von Krüger, W. C. A. Pereira, and E. E. C. Monteiro. Development of silicon-based materials for ultrasound biological phantoms. In *2009 IEEE International Ultrasonics Symposium*, pages 1962–1965.

[52] N. J. Maran and R. J. Glavin. Low- to high-fidelity simulation – a continuum of medical education? *Medical Education*, 37(s1):22–28, 2003.

[53] Robert Marcovich and Arthur D. Smith. Percutaneous renal access: tips and tricks. *BJU International*, 95(s2):78–84, 2005.

[54] Vitaly Margulis, D. Matsumoto Edward, E. Knudsen Bodo, H. Chew Ben, E. Pautler Stephen, A. Cadeddu Jeffrey, D. Denstedt John, and S. Pearle Margaret. 1162: Percutaneous renal collecting system access: Can virtual reality training shorten the learning curve? *Journal of Urology*, 173(4S):315–315, 2005.

[55] Christina Massoth, Hannah Röder, Hendrik Ohlenburg, Michael Hessler, Alexander Zarbock, Daniel M. Pöpping, and Manuel Wenk. High-fidelity is not superior to low-fidelity simulation but leads to overconfidence in medical students. *BMC Medical Education*, 19(1):29, 2019.

[56] D. Matsumoto Edward, E. Knudsen Bodo, H. Chew Ben, E. Pautler Stephen, D. Brooke Johnson, A. Cadeddu Jeffrey, D. Denstedt John, and S. Pearle Margaret. 1894: Impact of virtual reality (vr) simulator training on percutaneous renal collecting system access. *Journal of Urology*, 171(4S):500–500, 2004.

[57] Linda R. Elliott Michael D. Coovert. *Scaled worlds : development, validation, and applications / edited by Samuel G. Schiflett ... [et al.].* Ashgate, Aldershot, Hants, England ;, 2004.

[58] Shashikant Mishra, Abraham Kurien, Arvind Ganpule, Veeramani Muthu, Ravindra Sabnis, and Mahesh Desai. Percutaneous renal access training: content validation com-

parison between a live porcine and a virtual reality (vr) simulation model. *BJU International*, 106(11):1753–1756, 2010.

[59] Shashikant Mishra, Abraham Kurien, Rajesh Patel, Pradeep Patil, Arvind Ganpule, Veeramani Muthu, Bobby Ravindra, and Mahesh Desai. Validation of virtual reality simulation for percutaneous renal access training. *Journal of endourology / Endourological Society*, 24:635–40, 2010.

[60] Shashikant Mishra, Abraham Kurien, Rajesh Patel, Pradip Patil, Arvind Ganpule, Veeramani Muthu, Ravindra B. Sabnis, and Mahesh Desai. Validation of virtual reality simulation for percutaneous renal access training. *Journal of Endourology*, 24(4):635–640, 2010.

[61] Fadi Munshi, Hani Lababidi, and Sawsan Alyousef. Low- versus high-fidelity simulations in teaching and assessing clinical skills. *Journal of Taibah University Medical Sciences*, 10(1):12–15, 2015.

[62] Patricia K. Nguyen and Joseph C. Wu. Radiation exposure from imaging tests: is there an increased cancer risk? *Expert review of cardiovascular therapy*, 9(2):177–183, 2011.

[63] Yasser Noureldin, Nader Fahmy, Maurice Anidjar, and Sero Andonian. Is there a place for virtual reality simulators in assessment of competency in percutaneous renal access? *World Journal of Urology*, 34(5):733–739, 2016.

[64] Yasser A. Noureldin and Sero Andonian. Simulation for percutaneous renal access: Where are we? *Journal of Endourology*, 31(S1):S–10–S–19, 2016.

[65] Yasser A. Noureldin, Mohamed A. Elkoushy, and Sero Andonian. Assessment of percutaneous renal access skills during urology objective structured clinical examinations (osce). *Canadian Urological Association journal = Journal de l'Association des urologues du Canada*, 9(3-4):E104–E108, 2015.

[66] Yasser A. Noureldin, David M. Hoenig, Philip Zhao, Sammy E. Elsamra, Joshua Stern, Geoffrey Gaunay, Piruz Motamedinia, Zeph Okeke, Ardeshir R. Rastinehad, and Robert M. Sweet. Incorporation of the fluoroless c-arm trainer at the american urological association hands on training percutaneous renal access. *World Journal of Urology*, 36(7):1149–1155, 2018.

[67] Alessia Pacioni, Marina Carbone, Cinzia Freschi, Rosanna Viglialoro, Vincenzo Ferrari, and Mauro Ferrari. Patient-specific ultrasound liver phantom: materials and fabrication method. *International Journal of Computer Assisted Radiology and Surgery*, 10(7):1065–1075, 2015.

[68] Gili Palnizky, Sarel Halachmi, and Michal Barak. Pulmonary complications following percutaneous nephrolithotomy: A prospective study. *Current urology*, 7(3):113–116, 2013.

[69] Dharmesh Patel, Tamer El-Husseiny, Konstantinos Moraitis, Tawfiq Shaikh, Noor Buchholz, Junaid Masood, and Islam Junaid. 1332 assessing and developing percutaneous renal access skills of trainees using the state of the art perc mentor^{TM} simulation trainer. *Journal of Urology*, 183(4S):e514–e514, 2010.

[70] Terry M. Peters. Image-guidance for surgical procedures. *Physics in Medicine and Biology*, 51(14):R505–R540, 2006.

[71] Lauren H. Poniatowski, Sneha S. Somani, Domenico Veneziano, Sean McAdams, and Robert M. Sweet. Characterizing and simulating needle insertion forces for percutaneous renal access. *Journal of Endourology*, 30(10):1049–1055, 2016.

[72] Mark A. Preston, Brian D. M. Blew, Rodney H. Breau, Darren Beiko, Stuart J. Oake, and J. D. Watterson. Survey of senior resident training in urologic laparoscopy, robotics and endourology surgery in canada. *Canadian Urological Association journal = Journal de l'Association des urologues du Canada*, 4(1):42–46, 2010.

[73] Kathleen R. Rosen. The history of medical simulation. *Journal of Critical Care*, 23(2):157–166, 2008.

[74] Shakhawan Said, Ismaeel Aghaways, and Goran Fryad. Review of factors affecting total blood loss and need for blood transfusion in a series of patient undergoing unilateral percutaneous nephrolithotomy. *Urology & Nephrology Open Access Journal*, 3, 2016.

[75] Simpa S. Salami, Okeke Zeph, and Smith Arthur D. Percutaneous renal access. pages 1–5, 2013.

[76] Hoda Samia, Sadaf Khan, Justin Lawrence, and Conor P. Delaney. Simulation and its role in training. *Clinics in colon and rectal surgery*, 26(1):47–55, 2013.

[77] J. B. Sampaio Francisco, F. C. Zanier Jose, O. Afonso H. M. Aragã, and A. Favorito Luciano. Intrarenal access: 3-dimensional anatomical study. *Journal of Urology*, 148(6):1769–1773, 1992.

[78] Piyush Sarmah, Jim Voss, Adrian Ho, Domenico Veneziano, and Bhaskar Somani. Low vs. high fidelity: the importance of 'realism' in the simulation of a stone treatment procedure. *Current Opinion in Urology*, 27(4), 2017.

[79] Marlies P. Schijven and Jack J. Jakimowicz. Validation of virtual reality simulators: Key to the successful integration of a novel teaching technology into minimal access surgery. *Minimally Invasive Therapy & Allied Technologies*, 14(4/5):244–246, 2005.

[80] Neal E. Seymour. Vr to or: A review of the evidence that virtual reality simulation improves operating room performance. *World Journal of Surgery*, 32(2):182–188, 2008.

[81] Mohammad Shamim Khan, Kamran Ahmed, Andrea Gavazzi, Rishma Gohil, Libby Thomas, Johan Poulsen, Munir Ahmed, Peter Jaye, and Prokar Dasgupta. Development and implementation of centralized simulation training: evaluation of feasibility, acceptability and construct validity. *BJU International*, 111(3):518–523, 2013.

[82] Priyanka Singh, Lopa Sarkar, H. S. Sethi, and V. S. Gupta. A randomized controlled prospective study to assess the role of subconjunctival bevacizumab in primary pterygium surgery in indian patients. *Indian journal of ophthalmology*, 63(10):779–784, 2015.

[83] Maneesh Sinha and Venkatesh Krishnamoorthy. Use of a vegetable model as a training tool for pcnl puncture. *Indian journal of urology : IJU : journal of the Urological Society of India*, 31(2):156–159, 2015.

[84] A. Skolarikos, G. Alivizatos, and J. J. M. C. H. de la Rosette. Percutaneous nephrolithotomy and its legacy. *European Urology*, 47(1):22–28, 2005.

[85] Yan Song, YaNan Ma, YongSheng Song, and Xiang Fei. Evaluating the learning curve for percutaneous nephrolithotomy under total ultrasound guidance. *PloS one*, 10(8):e0132986–e0132986, 2015.

[86] Peter L. Steinberg, Michelle J. Semins, Shaun E. L. Wason, Brian R. Matlaga, and Vernon M. Pais. Fluoroscopy-guided percutaneous renal access. *Journal of Endourology*, 23(10):1627–1631, 2009.

[87] Walter Ludwig Strohmaier and Andreas Giese. Ex vivo training model for percutaneous renal surgery. *Urological Research*, 33(3):191–193, 2005.

[88] Walter Ludwig Strohmaier and Andreas Giese. Improved ex vivo training model for percutaneous renal surgery. *Urological Research*, 37(2):107, 2009.

[89] K. J. M. Surry, H. J. B. Austin, A. Fenster, and T. M. Peters. Poly(vinyl alcohol) cryogel phantoms for use in ultrasound and mr imaging. *Physics in medicine and biology*, 49(24):5529–5546, 2004.

[90] Yonghang Tai, Lei Wei, Hailing Zhou, Jun Peng, Qiong Li, Feiyan Li, Jun Zhang, and Junsheng Shi. Augmented-reality-driven medical simulation platform for percutaneous

nephrolithotomy with cybersecurity awareness. *International Journal of Distributed Sensor Networks*, 15(4), 2019.

[91] Ahmad M. Tawfik, Ahmed S. El-Abd, Mohamed Abo El-Enen, Yasser A. Farahat, Mohamed A. El-Bendary, Osama M. El-Gamal, Mohamed G. Soliman, Abdelhameed M. El-Bahnasy, and Mohamed Rasheed. Validity of a sponge trainer as a simple training model for percutaneous renal access. *Arab Journal of Urology*, 15(3):204–210, 2017.

[92] Eric Taylor, Joe Miller, Thomas Chi, and Marshall L. Stoller. Complications associated with percutaneous nephrolithotomy. *Translational andrology and urology*, 1(4):223–228, 2012.

[93] Jeffrey J. Tomaszewski, Tara D. Ortiz, Bishoy A. Gayed, Marc C. Smaldone, Stephen V. Jackman, and Timothy D. Averch. Renal access by urologist or radiologist during percutaneous nephrolithotomy. *Journal of Endourology*, 24(11):1733–1737, 2010.

[94] Toronto general hospital department of anesthesia perioperative interactive education. Ultrasonography basics. http://pie.med.utoronto.ca/OBAnesthesia/OBAnesthesia$_$content/OBA$_$ultrasonographyBasics$_$module.html, Last accessed on 2020-08-25.

[95] Benjamin W. Turney. A new model with an anatomically accurate human renal collecting system for training in fluoroscopy-guided percutaneous nephrolithotomy access. *Journal of endourology*, 28(3):360–363, 2014.

[96] Manint Usawachintachit, Selma Masic, Isabel E. Allen, Jianxing Li, and Thomas Chi. Adopting ultrasound guidance for prone percutaneous nephrolithotomy: Evaluating the learning curve for the experienced surgeon. *Journal of endourology*, 30(8):856–863, 2016.

[97] Manint Usawachintachit, David T. Tzou, Weiguo Hu, Jianxing Li, and Thomas Chi. X-ray-free ultrasound-guided percutaneous nephrolithotomy: How to select the right patient? *Urology*, 100:38–44, 2017.

[98] Michail Varras, Nikolaos Nikiteas, Viktoria-Konstantina Varra, Fani-Niki Varra, Evangelos Georgiou, and Constantinos Loukas. Role of laparoscopic simulators in the development and assessment of laparoscopic surgical skills in laparoscopic surgery and gynecology (review). *World Acad Sci J*, 2(2):65–76, 2020.

[99] Domenico Veneziano, Arthur Smith, Troy Reihsen, Jason Speich, and Robert M. Sweet. The simportal fluoro-less c-arm trainer: An innovative device for percutaneous kidney access. *Journal of Endourology*, 29(2):240–245, 2014.

[100] Mohankumar Vijayakumar, Sudharsan Balaji, Abhishek Singh, Arvind Ganpule, Ravindra Sabnis, and Mahesh Desai. A novel biological model for training in percutaneous renal access. *Arab journal of urology*, 17(4):292–297, 2019.

[101] D. Watterson James, Shawn Soon, and Kunal Jana. Access related complications during percutaneous nephrolithotomy: Urology versus radiology at a single academic institution. *Journal of Urology*, 176(1):142–145, 2006.

[102] W. Xia, E. C. S. Chen, S. E. Pautler, and T. M. Peters. A global optimization method for specular highlight removal from a single image. *IEEE Access*, 7:125976–125990, 2019.

[103] Yuyu Xu, Yaoji Yuan, Yichuan Cai, Xun Li, Shawpong Wan, and Guibin Xu. Use 3d printing technology to enhance stone free rate in single tract percutaneous nephrolithotomy for the treatment of staghorn stones. *Urolithiasis*, 2019.

[104] Weimin Yu, Ting Rao, Xing Li, Yuan Ruan, Run Yuan, Chenglong Li, Haoyong Li, and Fan Cheng. The learning curve for access creation in solo ultrasonography-guided percutaneous nephrolithotomy and the associated skills. *International Urology and Nephrology*, 49(3):419–424, 2017.

[105] Ali Akbar Zehri, Syed Raziuddin Biyabani, Khurram Muthair Siddiqui, and Amanullah Memon. Triggers of blood transfusion in percutaneous nephrolithotomy. *Journal of the College of Physicians and Surgeons–Pakistan : JCPSP*, 21(3):138–141, 2011.

[106] Y. Zhang, CF. Yu, SH. Jin, NC. Li, and YQ. Na. Validation of a novel non-biological bench model for the training of percutaneous renal access. *International braz j urol*, 40:87 – 92, 2014.

[107] Yi Zhang, Tong-wen Ou, Jian-guo Jia, Wei Gao, Xin Cui, Jiang-tao Wu, and Gang Wang. Novel biologic model for percutaneous renal surgery learning and training in the laboratory. *Urology*, 72(3):513–516, 2008.

[108] Yi Zhang, Cheng-fan Yu, Jin-shun Liu, Gang Wang, He Zhu, and Yan-qun Na. Training for percutaneous renal access on a virtual reality simulator. *Chinese Medical Journal*, 126(8), 2013.

[109] Q. I. U. Zhi, Yang Yong, Zhang Yi, and S. U. N. Yu-cheng. Modified biological training model for percutaneous renal surgery with ultrasound and fluroscopy guidance. *Chinese Medical Journal*, 124(9), 2011.

[110] Wei Zhu, Jiasheng Li, Jian Yuan, Yongda Liu, Shaw P. Wan, Guanzhao Liu, Wenzhong Chen, Wenqi Wu, Jintai Luo, Dongliang Zhong, Defeng Qi, Ming Lei, Wen Zhong, Ze Zhang, Zhaohui He, Zhijian Zhao, Suilin Lu, Yuji Wu, and Guohua Zeng. A prospective and randomised trial comparing fluoroscopic, total ultrasonographic, and combined guidance for renal access in mini-percutaneous nephrolithotomy. *BJU International*, 119(4):612–618, 2017.

Appendix A. Example of US Simulation Configuration File

```xml
<PlusConfiguration version="2.3">

  <DataCollection StartupDelaySec="1.0" >
    <DeviceSet
      Name="PlusServer For Unity local Moderate 2"
      Description="Simulated Ultrasound"
    />
     <!-- Image marker tracker-->
    <Device
      Id="TrackerDevice"
      Type="OpenIGTLinkTracker"
      MessageType="TRANSFORM"
      ToolReferenceFrame="Tracker"
      ServerAddress="127.0.0.1"
      ServerPort="18946"
      AcquisitionRate="90"
      IgtlMessageCrcCheckEnabled="true"
      UseReceivedTimestamps="false"
      UseLastTransformsOnReceiveTimeout="true"
      LocalTimeOffsetSec ="0.0"
      ReconnectOnReceiveTimeout="true">
      <DataSources>
        <DataSource Type="Tool" Id="Probe"  />
        <DataSource Type="Tool" Id="Needle"  />
        <DataSource Type="Tool" Id="Kidney" />
        <DataSource Type="Tool" Id="Gelblock" />
      </DataSources>
      <OutputChannels>
        <OutputChannel Id="TrackerStream">
          <DataSource Id="Probe" />
          <DataSource Id="Needle" />
          <DataSource Id="Kidney" />
          <DataSource Id="Gelblock" />
        </OutputChannel>
      </OutputChannels>
    </Device>
  <!-- For getting images from the US simulator -->
    <Device
      Id="VideoDevice"
      Type="UsSimulator"
      LocalTimeOffsetSec="0.0"
```

```xml
  AcquisitionRate="90" >
<DataSources>
  <DataSource Type="Video" Id="Video" PortUsImageOrientation="MF" />
</DataSources>
<InputChannels>
  <InputChannel Id="TrackerStream" />
</InputChannels>
<OutputChannels>
  <OutputChannel Id="VideoStream" VideoDataSourceId="Video" />
</OutputChannels>
<vtkPlusUsSimulatorAlgo
  ImageCoordinateFrame="Image"
  ReferenceCoordinateFrame="Reference"
  IncomingIntensityMwPerCm2="300"
  BrightnessConversionGamma="0.25"
  BrighntessConversionOffset="30"
  NumberOfScanlines="128"
  NumberOfSamplesPerScanline="1000"
  NoiseAmplitude="14.0"
  NoiseFrequency="2.5 3.5 1"
  NoisePhase="50 20 0"
  >
  <SpatialModel Name="Air"
  DensityKgPerM3="1.2"
  SoundVelocityMPerSec="343"
  AttenuationCoefficientDbPerCmMhz="100.0"
  BackscatterDiffuseReflectionCoefficient="0.1"
  SurfaceReflectionIntensityDecayDbPerMm="50"
  />
  <SpatialModel
    Name="Gelblock"
    Type="Model"
    ObjectCoordinateFrame="Gelblock"
    ModelFile="D:/AllModels/CubeModel_m.stl"
    DensityKgPerM3="910"
    SoundVelocityMPerSec="1540"
    AttenuationCoefficientDbPerCmMhz="3.0"
    BackscatterDiffuseReflectionCoefficient="0.1"
    SurfaceSpecularReflectionCoefficient="0.0"
    SurfaceDiffuseReflectionCoefficient="0.0"
    TransducerSpatialModelMaxOverlapMm="50"
  />
  <SpatialModel
    Name="Kidney"
    ObjectCoordinateFrame="Kidney"
```

```xml
    ModelFile="D:/AllModels/ModerateKidney2_m.stl"
    DensityKgPerM3="1066"
    SoundVelocityMPerSec="1570"
    AttenuationCoefficientDbPerCmMhz="1.0"
    BackscatterDiffuseReflectionCoefficient="0.001"
    SurfaceSpecularReflectionCoefficient="0.0"
    SurfaceDiffuseReflectionCoefficient="0.0" />
<SpatialModel
    Name="Calyces"
    ObjectCoordinateFrame="Kidney"
    ModelFile="D:/AllModels/ModerateCollecting2_m.stl"
    DensityKgPerM3="1201"
    SoundVelocityMPerSec="2200"
    AttenuationCoefficientDbPerCmMhz="0"
    BackscatterDiffuseReflectionCoefficient="0.000"
    SurfaceSpecularReflectionCoefficient="0.0"
    SurfaceDiffuseReflectionCoefficient="0.3"
/>
<!--SpatialModel
    Name="Vessel"
    ObjectCoordinateFrame="Kidney"
    ModelFile="D:/Artery_m.stl"
    ModelToObjectTransform="
      1 0 0 0
      0 1 0 0
      0 0 1 0
      0 0 0 1"
    DensityKgPerM3="1102"
    SoundVelocityMPerSec="2000"
    AttenuationCoefficientDbPerCmMhz="0.01"
    BackscatterDiffuseReflectionCoefficient="0.001"
    SurfaceSpecularReflectionCoefficient="0.0"
    SurfaceDiffuseReflectionCoefficient="0.0"
/-->

<SpatialModel
    Name="Needle"
    ObjectCoordinateFrame="NeedleTip"
    ModelFile="D:/AllModels/NeedleModel.stl"
    DensityKgPerM3="2500"
    SoundVelocityMPerSec="5000"
    AttenuationCoefficientDbPerCmMhz="3.0"
    BackscatterDiffuseReflectionCoefficient="1"
    SurfaceSpecularReflectionCoefficient="0.0"
    SurfaceDiffuseReflectionCoefficient="0.3"
```

```xml
            SurfaceReflectionIntensityDecayDbPerMm="0.1"
          />
          <SpatialModel
            Name="Needle"
            ObjectCoordinateFrame="NeedleTip"
            ModelFile="D:/AllModels/NeedleModel_Double_6mm.stl"
            DensityKgPerM3="1600"
            SoundVelocityMPerSec="5000"
            AttenuationCoefficientDbPerCmMhz="0.03"
            BackscatterDiffuseReflectionCoefficient="0.9"
            SurfaceSpecularReflectionCoefficient="0.0"
            SurfaceDiffuseReflectionCoefficient="0.0"
            SurfaceReflectionIntensityDecayDbPerMm="0"
          />
          <RfProcessing>
            <ScanConversion
              TransducerName="Ultrasonix_C5-2/60"
              TransducerGeometry="CURVILINEAR"
              ModelToObjectTransform="
              1 0 0 0
              0 1 0 0
              0 0 1 0
              0 0 0 1"
              RadiusStartMm="60.0"
              RadiusStopMm="130.0"
              ThetaStartDeg="-28.0"
              ThetaStopDeg="28.0"
              TransducerCenterPixel="410 100"
              OutputImageSizePixel="820 616"
              OutputImageSpacingMmPerPixel="0.13 0.13" />
          </RfProcessing>
          <!-
- Image size pixel change background black size  small: smaller black window  -->
          <!-
- Image pixel spacing change ultrasound simulation size  larger spacing: smaller
US image affects resolution -->
        </vtkPlusUsSimulatorAlgo>

    </Device>

    <Device
      Id="TrackedVideoDevice"
      Type="VirtualMixer" >
      <InputChannels>
        <InputChannel Id="TrackerStream" />
```

```xml
        <InputChannel Id="VideoStream" />
      </InputChannels>

      <OutputChannels>
        <OutputChannel Id="TrackedVideoStream"/>
      </OutputChannels>
    </Device>

    <!--Device
      Id="CaptureDevice"
      Type="VirtualCapture"
      BaseFilename="RecordingTest.igs.mhd"
      EnableCapturingOnStart="FALSE"  >
      <InputChannels>
        <InputChannel Id="TrackedVideoStream" />
      </InputChannels>
    </Device-->
  </DataCollection>

  <PlusOpenIGTLinkServer
    MaxNumberOfIgtlMessagesToSend="10"
    MaxTimeSpentWithProcessingMs="50"
    ListeningPort="18944"
    SendValidTransformsOnly="true"
    OutputChannelId="TrackedVideoStream" >
    <DefaultClientInfo>
      <MessageTypes>
        <Message Type="IMAGE" />
        <Message Type="TRANSFORM" />
      </MessageTypes>
      <TransformNames>
      <!--These transforms becomes active transforms in slicer-->
        <Transform Name="GelblockToReference" />
        <Transform Name="NeedleTipToReference" />
        <Transform Name="ProbeToReference" />
        <Transform Name="KidneyToReference" />
      </TransformNames>
      <ImageNames>
        <Image Name="Image" EmbeddedTransformToFrame="Reference" />
      </ImageNames>
    </DefaultClientInfo>
  </PlusOpenIGTLinkServer>

  <CoordinateDefinitions>
  <!--scaling change 1xX -->
```

```xml
    <Transform From="Image" To="Probe"
    Matrix="
            0.13 0 0 -53.3
            0 0 0.13 0
            0 -0.13 0 8
            0 0 0 1" />

    <Transform From="Image" To="TransducerOriginPixel"
      Matrix="
            1 0 0 0
            0 1 0 0
            0 0 1 0
            0 0 0 1" />
    <Transform From="Tracker" To="Reference"
      Matrix="
            1 0 0 0
            0 1 0 0
            0 0 1 0
            0 0 0 1"  />
    <Transform From="NeedleTip" To="Needle"
      Matrix="
           1 0 0 0
           0 1 0 0
           0 0 1 0
           0 0 0 1" />

  </CoordinateDefinitions>

</PlusConfiguration>
```

Appendix B. UNITY C# Marshalling

```csharp
using System.Collections;
using System.Collections.Generic;
using UnityEngine;
using System.Runtime.InteropServices;
using UnityEngine.UI;
using System;
using System.IO;
using System.Net.Sockets;
using AOT;
using System.Threading;
using UnityEngine.SceneManagement;

public class UnityIGT : MonoBehaviour
{

    private delegate void ServerDelegate(int Svalue);
    [DllImport("OpenIGTLink")]
    static extern void ServerConnect(int serverport, double fps, ServerDelegate
ServerConnectionStatus);


    private delegate void ReceiverDelegate(int Rvalue);
    [DllImport("OpenIGTLink")]
    static extern void ReceiverConnect(string hostname, int clientport, ReceiverDelegate
ReceiverConnectionStatus);


    private delegate void PositionDelegate(float PositionX);
    [DllImport("OpenIGTLink")]
    static extern void GetData(float[] orientation, int Osize, float[] position, int
Psize, PositionDelegate SentPosition);


    private delegate void GetImageDelegate(IntPtr Address);
    [DllImport("OpenIGTLink")]
    static extern void GetImage(GetImageDelegate GetImageData);

    private delegate void CloseSendDelegate();
    [DllImport("OpenIGTLink")]
    static extern void CloseSendSocket();

    private delegate void CloseReceiveDelegate();
    [DllImport("OpenIGTLink")]
    static extern void CloseReceiveSocket();



    public GameObject[] TracketObject;
    float[] ObjectPosition = new float[12];
    float[] ObjectOrientation = new float[16];
    public static GameObject MySprite;
    public static GameObject MySpriteSM;
    public InputField EnterIP;
```

```csharp
    string IPAddress;
    bool startR = false;
    bool startS = false;
    static bool Received = false;
    public static byte[] ImageData;
    public static Texture2D ImageTexture;
    Thread ReceiveThread;
    Thread SendThread;

    public static Text Statustext; //disconnect/connect/receiver


    void Start()
    {
        MySprite = GameObject.FindWithTag("Image");
        MySpriteSM = GameObject.FindWithTag("SmallImage");
        Application.targetFrameRate = 60;
        ImageData = new byte[505120];
    }


    void Update()
    {
        for (int i = 0; i < 4; i++)
        {
            if (TracketObject[i].activeSelf == true)
            {
                //ObjectStatustext.text = "Object Found";
                ObjectPosition[i * 3 + 0] = TracketObject[i].transform.position.x;
                ObjectPosition[i * 3 + 1] = TracketObject[i].transform.position.y;
                ObjectPosition[i * 3 + 2] = TracketObject[i].transform.position.z;
                ObjectOrientation[i * 4 + 0] = TracketObject[i].transform.rotation.x;
                ObjectOrientation[i * 4 + 1] = TracketObject[i].transform.rotation.y;
                ObjectOrientation[i * 4 + 2] = TracketObject[i].transform.rotation.z;
                ObjectOrientation[i * 4 + 3] = TracketObject[i].transform.rotation.w;
            }
            else
            {
                //ObjectStatustext.text = "Object Lost";
                Array.Clear(array: ObjectPosition, index: 0, length:
ObjectPosition.Length);
                Array.Clear(array: ObjectOrientation, index: 0, length:
ObjectOrientation.Length);
            }
        }
        Resources.UnloadUnusedAssets();

    }


    public void StartServer()
    {
        ServerConnect(18946, 60, ServerConnectionStatus);
    }
    public void StartClient()
    {
        IPAddress = EnterIP.text;
        ReceiverConnect(IPAddress, 18944, ReceiverConnectionStatus);
```

```csharp
}
public void AutoSend()
{
    InvokeRepeating("StartSendData", 0f, 0.03333f);


}
public void StartSendData()
{
    GetData(ObjectOrientation, 4, ObjectPosition, 3, SentPosition);
}

public void StartReceiveThread()
{
    startR = true;
    ReceiveThread = new Thread(AutoReceive);
    ReceiveThread.Start();
}
public void AutoReceive()
{
    while (startR == true)
    {
        StartReceivingImage();
    }
}
public void StartReceivingImage()
{
    GetImage(GetImageDataAddress);
}
public void InvokeUpdate()
{
    InvokeRepeating("UpdateTexture", 0f, 0.033333f);
}
public void UpdateTexture()
{
    if (Received == true)
    {
        ImageTexture = new Texture2D(820, 616, TextureFormat.Alpha8, false);
        ImageTexture.LoadRawTextureData(ImageData);
        ImageTexture.Apply();
        MySprite.GetComponent<RawImage>().texture = ImageTexture;
        MySpriteSM.GetComponent<RawImage>().texture = ImageTexture;
    }
}


[MonoPInvokeCallback(typeof(ServerDelegate))]
private static void ServerConnectionStatus(int Svalue)
{
    if (Svalue == 1)
    {
        Statustext = GameObject.FindWithTag("Status").GetComponent<Text>();
        Statustext.text = "Connected to Server";
    }
}
[MonoPInvokeCallback(typeof(ReceiverDelegate))]
private static void ReceiverConnectionStatus(int Rvalue)
{
    if (Rvalue == 1)
    {
```

```csharp
        {
            Statustext = GameObject.FindWithTag("Status").GetComponent<Text>();
            Statustext.text = "Receiver Started";
        }
    }
    [MonoPInvokeCallback(typeof(PositionDelegate))]
    private static void SentPosition(float PositionX) //verify plus received position
    {
    }
    [MonoPInvokeCallback(typeof(GetImageDelegate))]
    private static void GetImageDataAddress(IntPtr Address)
    {
        Marshal.Copy(Address, ImageData, 0, 505120);
        Received = true;
        //RC = RC + 1;
    }
    public void LetsGo()
    {
        AutoSend();
        StartClient();
        StartReceiveThread();
        InvokeUpdate();
    }
    public void Restart()
    {
        ReceiveThread.Abort();
        SceneManager.LoadScene("UltrasoundSimulator_Standing_Sep");
    }

    public void Disconnect()
    {
        startR = false;
        CloseReceiveSocket();
        CloseSendSocket();
        ReceiveThread.Abort();
    }
    private void OnApplicationQuit()
    {
        ReceiveThread.Abort();
    }

}
```

Appendix C. OpenIGTLink Based Sender

```cpp
#include <iomanip>
#include <iostream>
#include <math.h>
#include <cstdlib>
#include <cstdlib>

#include "igtlOSUtil.h"
#include "igtlMessageHeader.h"
#include "igtlTransformMessage.h"
#include "igtlServerSocket.h"
#include "igtlClientSocket.h"
#include "igtlTrackingDataMessage.h"
#include "igtl_tdata.h"

#define UnityIGTLinkSendAPI _declspec(dllexport)

igtl::ServerSocket::Pointer  UnityServerSocket;
igtl::Socket::Pointer UnitySendSocket;
igtl::TimeStamp::Pointer ts;

extern "C" {
    typedef void(_stdcall* CallbackServer)(int Svalue);
    UnityIGTLinkSendAPI void _stdcall ServerConnect(int serverport, double fps,
CallbackServer ServerConnectionStatus)
        //UnityIGTLinkSendAPI void ServerConnect(int serverport, double fps,
void(*ServerConnectionStatus)(int Svalue))
    {

        //int interval = (int)(1000.0 / fps);

        // Establish Connection
        igtl::ServerSocket::Pointer serversocket;
        serversocket = igtl::ServerSocket::New();
        int r = serversocket->CreateServer(serverport);
        UnityServerSocket = serversocket;
        UnitySendSocket = serversocket->WaitForConnection(10000);

        if (UnitySendSocket.IsNotNull())
        {
            ServerConnectionStatus(1);
        }

    }
    //---------------------------------------------------------------------------
    ---------------------------------------

    void SendProbeToReference(igtl::Matrix4x4& Pmatrix, igtl::ServerSocket::Pointer
serversocket, igtl::Socket::Pointer clientsocket)
    {
        // Allocate Transform Message Class
        igtl::TransformMessage::Pointer PTransformMessage =
igtl::TransformMessage::New();

        //Package Data then send
```

```cpp
		PTransformMessage->SetHeaderVersion(IGTL_HEADER_VERSION_1);
		PTransformMessage->InitPack();
		PTransformMessage->SetDeviceName("ProbeToTracker");
		PTransformMessage->SetMatrix(Pmatrix);
		ts = igtl::TimeStamp::New();
		ts->GetTime();
		PTransformMessage->SetTimeStamp(ts);
		PTransformMessage->Pack();
		UnitySendSocket->Send(PTransformMessage->GetPackPointer(),
PTransformMessage->GetPackSize());
		//igtl::Sleep(1); // wait
	// Close connection
  //socket->CloseSocket();
	}
	UnityIGTLinkSendAPI void _stdcall CloseSendSocket()
	{
		UnityServerSocket->CloseSocket();
		UnitySendSocket->CloseSocket();
	}
	//-----------------------------------------------------------
	void SendNeedleToReference(igtl::Matrix4x4& Nmatrix, igtl::ServerSocket::Pointer
serversocket, igtl::Socket::Pointer clientsocket)
	{
	 // Allocate Transform Message Class
		igtl::TransformMessage::Pointer NTransformMessage =
igtl::TransformMessage::New();
		//Package Data then send
		NTransformMessage->SetHeaderVersion(IGTL_HEADER_VERSION_1);
		NTransformMessage->InitPack();
		NTransformMessage->SetDeviceName("NeedleToTracker");
		NTransformMessage->SetMatrix(Nmatrix);
		ts = igtl::TimeStamp::New();
		ts->GetTime();
		NTransformMessage->SetTimeStamp(ts);
		NTransformMessage->Pack();
		UnitySendSocket->Send(NTransformMessage->GetPackPointer(),
NTransformMessage->GetPackSize());
		//igtl::Sleep(1); // wait
	// Close connection
	//socket->CloseSocket();
	}
	//-----------------------------------------------------------
	void SendKidneyToReference(igtl::Matrix4x4& Kmatrix, igtl::ServerSocket::Pointer
serversocket, igtl::Socket::Pointer clientsocket)
	{
	 // Allocate Transform Message Class
		igtl::TransformMessage::Pointer KTransformMessage =
igtl::TransformMessage::New();
		//Package Data then send
		KTransformMessage->SetHeaderVersion(IGTL_HEADER_VERSION_1);
		KTransformMessage->InitPack();
		KTransformMessage->SetDeviceName("KidneyToTracker");
		KTransformMessage->SetMatrix(Kmatrix);
		ts = igtl::TimeStamp::New();
		ts->GetTime();
		KTransformMessage->SetTimeStamp(ts);
		KTransformMessage->Pack();
```

```cpp
            UnitySendSocket->Send(KTransformMessage->GetPackPointer(),
KTransformMessage->GetPackSize());
            //igtl::Sleep(1); // wait
      // Close connection
          //socket->CloseSocket();
      }
      void SendGelblockToReference(igtl::Matrix4x4& Gmatrix, igtl::ServerSocket::Pointer
serversocket, igtl::Socket::Pointer clientsocket)
      {
            // Allocate Transform Message Class
            igtl::TransformMessage::Pointer GTransformMessage =
igtl::TransformMessage::New();
            //Package Data then send
            GTransformMessage->SetHeaderVersion(IGTL_HEADER_VERSION_1);
            GTransformMessage->InitPack();
            GTransformMessage->SetDeviceName("GelblockToTracker");
            GTransformMessage->SetMatrix(Gmatrix);
            ts = igtl::TimeStamp::New();
            ts->GetTime();
            GTransformMessage->SetTimeStamp(ts);
            GTransformMessage->Pack();
            UnitySendSocket->Send(GTransformMessage->GetPackPointer(),
GTransformMessage->GetPackSize());
            //igtl::Sleep(1); // wait
            // Close connection
            //socket->CloseSocket();
      }
      //------------------------------------------------------------------------------
------------------------------------------
      typedef void(_stdcall* CallbackPosition)(float ReceivedPosition);
      UnityIGTLinkSendAPI void _stdcall GetData(float *Rorientation, int Osize, float
*Rposition, int Psize, CallbackPosition CheckPosition)
      //UnityIGTLinkSendAPI void GetData(float *Rorientation, int Osize, float
*Rposition, int Psize, void(*CheckPosition)(float ReceivedPosition))
      {

            // build matrx
            igtl::Matrix4x4 Pmatrix;
            float Porientation[] =
{ Rorientation[0],Rorientation[1],Rorientation[2],Rorientation[3] };
            igtl::QuaternionToMatrix(Porientation, Pmatrix);
            Pmatrix[0][3] = Rposition[0];
            Pmatrix[1][3] = Rposition[1];
            Pmatrix[2][3] = Rposition[2];

            igtl::Matrix4x4 Nmatrix;
            float Norientation[] =
{ Rorientation[4],Rorientation[5],Rorientation[6],Rorientation[7] };
            igtl::QuaternionToMatrix(Norientation, Nmatrix);
            Nmatrix[0][3] = Rposition[3];
            Nmatrix[1][3] = Rposition[4];
            Nmatrix[2][3] = Rposition[5];

            igtl::Matrix4x4 Kmatrix;
            float Korientation[] =
{ Rorientation[8],Rorientation[9],Rorientation[10],Rorientation[11] };
            igtl::QuaternionToMatrix(Korientation, Kmatrix);
            Kmatrix[0][3] = Rposition[6];
```

```cpp
            Kmatrix[1][3] = Rposition[7];
            Kmatrix[2][3] = Rposition[8];

            igtl::Matrix4x4 Gmatrix;
            float Gorientation[] =
{ Rorientation[12],Rorientation[13],Rorientation[14],Rorientation[15] };
            igtl::QuaternionToMatrix(Gorientation, Gmatrix);
            Gmatrix[0][3] = Rposition[9];
            Gmatrix[1][3] = Rposition[10];
            Gmatrix[2][3] = Rposition[11];

            float receivedX = Nmatrix[0][3];
        CheckPosition(receivedX);

            SendProbeToReference(Pmatrix, UnityServerSocket, UnitySendSocket);
            SendNeedleToReference(Nmatrix, UnityServerSocket, UnitySendSocket);
            SendKidneyToReference(Kmatrix, UnityServerSocket, UnitySendSocket);
            SendGelblockToReference(Gmatrix, UnityServerSocket, UnitySendSocket);
        }

    //-------------------------------------------------------------------------------
-------------------------------------

}
```

Appendix D. OpenIGTLink Based Receiver

```cpp
#include <iomanip>
#include <iostream>
#include <math.h>
#include <cstdlib>

#include "igtlOSUtil.h"
#include "igtlMessageHeader.h"
#include "igtlTransformMessage.h"
#include "igtlServerSocket.h"
#include "igtlClientSocket.h"
#include "igtlTrackingDataMessage.h"
#include "igtl_tdata.h"
#include "igtlImageMessage.h"
#include "igtlStatusMessage.h"

#define UnityIGTLinkReceiveAPI _declspec(dllexport)

igtl::ImageMessage::Pointer SendimgMsg;
igtl::ClientSocket::Pointer Unityclientsocket;

extern "C" {
        typedef void(_stdcall* CallbackImage)(void* ImageDataPointer);
        UnityIGTLinkReceiveAPI void _stdcall GetImage(CallbackImage GetImageData)
                //----------------------------------------------------------------------
--
        {

                // Create a message buffer to receive header
                igtl::MessageHeader::Pointer headerMsg;
                headerMsg = igtl::MessageHeader::New();
                //------------------------------------------------------------
                // Allocate a time stamp
                igtl::TimeStamp::Pointer ts;
                ts = igtl::TimeStamp::New();
                //------------------------------------------------------------
                //for (int i = 0; i < 100; i++)
                //{
                // Initialize receive buffer
                headerMsg->InitPack();
                // Receive generic header from the socket
                int r = Unityclientsocket->Receive(headerMsg->GetPackPointer(),
headerMsg->GetPackSize());
                headerMsg->Unpack();
                //------------------------------------------------------------
                // Get time stamp
                igtlUint32 sec;
                igtlUint32 nanosec;
                headerMsg->GetTimeStamp(ts);
                ts->GetTimeStamp(&sec, &nanosec);

                // Check data type and receive data body
                if (strcmp(headerMsg->GetDeviceType(), "IMAGE") == 0)
                {

                        igtl::ImageMessage::Pointer imgMsg;
```

```cpp
                imgMsg = igtl::ImageMessage::New();
                imgMsg->SetMessageHeader(headerMsg);
                imgMsg->AllocatePack();
                // Receive transform data from the socket
                Unityclientsocket->Receive(imgMsg->GetPackBodyPointer(),
imgMsg->GetPackBodySize());
                // Deserialize the transform data
                // If you want to skip CRC check, call Unpack() without argument.
                int c = imgMsg->Unpack(0);
                if (c & igtl::MessageHeader::UNPACK_BODY) // if CRC check is OK
                {
                        // Retrive the image data
                        int   size[3];          // image dimension
                        float spacing[3];       // spacing (mm/pixel)
                        int   svsize[3];        // sub-volume size
                        int   svoffset[3];      // sub-volume offset
                        int   scalarType;       // scalar type
                        int   endian;           // endian

                        scalarType = imgMsg->GetScalarType();
                        endian = imgMsg->GetEndian();
                        imgMsg->GetDimensions(size);
                        imgMsg->GetSpacing(spacing);
                        imgMsg->GetSubVolume(svsize, svoffset);
                        imgMsg->AllocateScalars();
                        imgMsg->GetScalarPointer();
                        GetImageData(imgMsg->GetScalarPointer());
                }
        }
        else
        {
                Unityclientsocket->Skip(headerMsg->GetBodySizeToRead(), 0);
        }

    }
    typedef void(_stdcall* CallbackReceiver)(int Cvalue);
    UnityIGTLinkReceiveAPI void _stdcall ReceiverConnect(char*  hostname, int
clientport, CallbackReceiver ReceiverConnectionStatus)
            //UnityIGTLinkReceiveAPI void ReceiverConnect(char*  hostname, int
clientport, void(*ReceiverConnectionStatus)(int Cvalue))
    {
            igtl::ClientSocket::Pointer clientsocket;
            clientsocket = igtl::ClientSocket::New();
            int j = clientsocket->ConnectToServer(hostname, clientport);
            Unityclientsocket = clientsocket;

            if (j == 0)
            {
                    ReceiverConnectionStatus(1);
            }

            //-----------------------------------------------------------
            // Close connection (The example code never reaches this section ...)
            // clientsocket->CloseSocket();
    }
    UnityIGTLinkReceiveAPI void _stdcall CloseReceiveSocket()
    {
            Unityclientsocket->CloseSocket();
```

```
        }
}
```

SPRINGER NATURE LICENSE
TERMS AND CONDITIONS

Nov 10, 2020

This Agreement between ▮▮▮▮▮▮▮▮▮▮ ("You") and Springer Nature ("Springer Nature")
consists of your license details and the terms and conditions provided by Springer Nature
and Copyright Clearance Center.

License Number	4945600486047
License date	Nov 10, 2020
Licensed Content Publisher	Springer Nature
Licensed Content Publication	International Journal of Computer Assisted Radiology and Surgery
Licensed Content Title	Augmented reality simulator for ultrasound-guided percutaneous renal access
Licensed Content Author	▮▮▮▮▮▮▮▮▮▮
Licensed Content Date	Apr 20, 2020
Type of Use	Thesis/Dissertation
Requestor type	academic/university or research institute
Format	print and electronic
Portion	full article/chapter
Will you be	no

translating?

Circulation/distribution 1 - 29

Author of this Springer
Nature content   yes

Title   DEVELOPMENT AND VALIDATION OF AUGMENTED
                  REALITYTRAINING SIMULATOR FOR ULTRASOUND
                  GUIDEDPERCUTANEOUS RENAL ACCESS

Institution name   Western University

Expected presentation   Nov 2020
date

Requestor Location

Total   0.00 CAD

Terms and Conditions

you are requesting is original to the Licensor and does not carry the copyright of another entity (as credited in the published version).

1. 3. If the credit line on any part of the material you have requested indicates that it was reprinted or adapted with permission from another source, then you should also seek permission from that source to reuse the material.

2. Scope of Licence

2. 1. You may only use the Licensed Content in the manner and to the extent permitted by these Ts&Cs and any applicable laws.

2. 2. A separate licence may be required for any additional use of the Licensed Material, e.g. where a licence has been purchased for print only use, separate permission must be obtained for electronic re-use. Similarly, a licence is only valid in the language selected and does not apply for editions in other languages unless additional translation rights have been granted separately in the licence. Any content owned by third parties are expressly excluded from the licence.

2. 3. Similarly, rights for additional components such as custom editions and derivatives require additional permission and may be subject to an additional fee. Please apply to ███ for these rights.

2. 4. Where permission has been granted **free of charge** for material in print, permission may also be granted for any electronic version of that work, provided that the material is incidental to your work as a whole and that the electronic version is essentially equivalent to, or substitutes for, the print version.

2. 5. An alternative scope of licence may apply to signatories of the STM Permissions Guidelines, as amended from time to time.

3. Duration of Licence

3. 1. A licence for is valid from the date of purchase ('Licence Date') at the end of the relevant period in the below table:

Scope of Licence	Duration of Licence
Post on a website	12 months
Presentations	12 months
Books and journals	Lifetime of the edition in the language purchased

4. Acknowledgement

4. 1. The Licensor's permission must be acknowledged next to the Licenced Material in print. In electronic form, this acknowledgement must be visible at the same time as the figures/tables/illustrations or abstract, and must be hyperlinked to the journal/book's homepage. Our required acknowledgement format is in the Appendix below.

5. Restrictions on use

5. 1. Use of the Licensed Material may be permitted for incidental promotional use and minor editing privileges e.g. minor adaptations of single figures, changes of format, colour and/or style where the adaptation is credited as set out in Appendix 1 below. Any other changes including but not limited to, cropping, adapting, omitting material that affect the meaning, intention or moral rights of the author are strictly prohibited.

5. 2. You must not use any Licensed Material as part of any design or trademark.

5. 3. Licensed Material may be used in Open Access Publications (OAP) before publication by Springer Nature, but any Licensed Material must be removed from OAP sites prior to final publication.

6. Ownership of Rights

6. 1. Licensed Material remains the property of either Licensor or the relevant third party and any rights not explicitly granted herein are expressly reserved.

7. Warranty

IN NO EVENT SHALL LICENSOR BE LIABLE TO YOU OR ANY OTHER PARTY OR ANY OTHER PERSON OR FOR ANY SPECIAL, CONSEQUENTIAL, INCIDENTAL OR INDIRECT DAMAGES, HOWEVER CAUSED, ARISING OUT OF OR IN CONNECTION WITH THE DOWNLOADING, VIEWING OR USE OF THE MATERIALS REGARDLESS OF THE FORM OF ACTION, WHETHER FOR BREACH OF CONTRACT, BREACH OF WARRANTY, TORT, NEGLIGENCE, INFRINGEMENT OR OTHERWISE (INCLUDING, WITHOUT LIMITATION, DAMAGES BASED ON LOSS OF PROFITS, DATA, FILES, USE, BUSINESS OPPORTUNITY OR CLAIMS OF THIRD PARTIES), AND
WHETHER OR NOT THE PARTY HAS BEEN ADVISED OF THE POSSIBILITY OF SUCH DAMAGES. THIS LIMITATION SHALL APPLY NOTWITHSTANDING ANY FAILURE OF ESSENTIAL PURPOSE OF ANY LIMITED REMEDY PROVIDED HEREIN.

8. Limitations

8. 1. _BOOKS ONLY:_ Where **'reuse in a dissertation/thesis'** has been selected the following terms apply: Print rights of the final author's accepted manuscript (for clarity, NOT the published version) for up to 100 copies, electronic rights for use only on a personal website or institutional repository as defined by the Sherpa guideline (www.sherpa.ac.uk/romeo/).

9. Termination and Cancellation

9. 1. Licences will expire after the period shown in Clause 3 (above).

9. 2. Licensee reserves the right to terminate the Licence in the event that payment is not received in full or if there has been a breach of this agreement by you.

Appendix 1 — Acknowledgements:

For Journal Content:
Reprinted by permission from [**the Licensor**]: [**Journal Publisher** (e.g. Nature/Springer/Palgrave)] [**JOURNAL NAME**] [**REFERENCE CITATION** (Article name, Author(s) Name), [**COPYRIGHT**] (year of publication)

For **Advance Online Publication papers:**
Reprinted by permission from [**the Licensor**]: [**Journal Publisher** (e.g. Nature/Springer/Palgrave)] [**JOURNAL NAME**] [**REFERENCE CITATION** (Article name, Author(s) Name), [**COPYRIGHT**] (year of publication), advance online publication, day month year (doi: 10.1038/sj.[JOURNAL ACRONYM].)

For Adaptations/Translations:
Adapted/Translated by permission from [**the Licensor**]: [**Journal Publisher** (e.g. Nature/Springer/Palgrave)] [**JOURNAL NAME**] [**REFERENCE CITATION** (Article name, Author(s) Name), [**COPYRIGHT**] (year of publication)

Note: For any republication from the British Journal of Cancer, the following credit line style applies:

Reprinted/adapted/translated by permission from [**the Licensor**]: on behalf of Cancer Research UK: : [**Journal Publisher** (e.g. Nature/Springer/Palgrave)] [**JOURNAL NAME**] [**REFERENCE CITATION** (Article name, Author(s) Name), [**COPYRIGHT**] (year of publication)

For **Advance Online Publication** papers:
Reprinted by permission from The [**the Licensor**]: on behalf of Cancer Research UK: [**Journal Publisher** (e.g. Nature/Springer/Palgrave)] [**JOURNAL NAME**] [**REFERENCE CITATION** (Article name, Author(s) Name), [**COPYRIGHT**] (year of publication), advance online publication, day month year (doi: 10.1038/sj.[JOURNAL ACRONYM])

For Book content:
Reprinted/adapted by permission from [**the Licensor**]: [**Book Publisher** (e.g. Palgrave Macmillan, Springer etc) [**Book Title**] by [**Book author**(s)] [**COPYRIGHT**] (year of publication)

Other Conditions:

Version 1.2

From: ███████████

Sent: Wednesday, November 11, 2020 10:02 AM

To: ███████████

Subject: RE: Permission to Use Copyrighted Material in a Master's Thesis

███████████

Copyright permission is granted for this request to include Figure 5 from the article by Steinberg et al, published in JOURNAL OF ENDOUROLOGY in your thesis. Please give proper credit to the journal and to the publisher,

Kind regards,

███████████

From: ███████████

Sent: Tuesday, November 10, 2020 8:44 PM

To: ███████████

Subject: Permission to Use Copyrighted Material in a Master's Thesis

Dear:

I am a University of Western Ontario graduate student completing my Master's thesis entitled "DEVELOPMENT AND VALIDATION OF AUGMENTED REALITYTRAINING SIMULATOR FOR ULTRASOUND GUIDEDPERCUTANEOUS RENAL ACCESS". My thesis will be available in full-text on the internet for reference, study and / or copy. Except in situations where a thesis is under embargo or restriction, the electronic version will be accessible through the Western Libraries web pages, the Library's web catalogue, and also through web search engines. I will also be granting Library and Archives Canada and ProQuest/UMI a non-exclusive license to reproduce, loan, distribute, or sell single copies of my thesis by any means and in any form or format. These rights will in no way restrict republication of the material in any other form by you or by others authorized by you.

I would like permission to allow inclusion of the following material in my thesis:

FIG. 5. Needle advanced toward left renal lower-pole calix using triangulation technique, C-arm in oblique projection.

Fluoroscopy-Guided Percutaneous Renal Access

Publication: Journal of Endourology

Publisher: Mary Ann Liebert, Inc.

Date: Oct 1, 2009

The material will be attributed through a citation.

Please confirm in writing or by email that these arrangements meet with your approval.

Sincerely

██████████

WOLTERS KLUWER HEALTH, INC. LICENSE
TERMS AND CONDITIONS

Nov 12, 2020

This Agreement between█████████████████████and Wolters Kluwer Health, Inc.
("Wolters Kluwer Health, Inc.") consists of your license details and the terms and conditions
provided by Wolters Kluwer Health, Inc. and Copyright Clearance Center.

License Number	4946370158599
License date	Nov 12, 2020
Licensed Content Publisher	Wolters Kluwer Health, Inc.
Licensed Content Publication	WK Health Book
Licensed Content Title	A Practical Approach to Regional Anesthesiology and Acute Pain Medicine
Licensed Content Author	████████████████████████████████
Licensed Content Date	Oct 4, 2017
Type of Use	Dissertation/Thesis
Requestor type	University/College
Sponsorship	No Sponsorship
Format	Print and electronic
Will this be posted online?	Yes, on a secure website

Portion	Figures/tables/illustrations
Number of figures/tables/illustrations	1
Author of this Wolters Kluwer article	No
Will you be translating?	No
Intend to modify/change the content	No
Current or previous edition of book	Current edition
Title	DEVELOPMENT AND VALIDATION OF AUGMENTED REALITYTRAINING SIMULATOR FOR ULTRASOUND GUIDEDPERCUTANEOUS RENAL ACCESS
Institution name	Western University
Expected presentation date	Nov 2020
Portions	Figure 3.1
Requestor Location	
Total	0.00 CAD
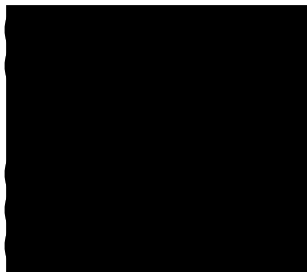
Terms and Conditions

1. **Duration of License:** Permission is granted for a one time use only. Rights herein do not apply to future reproductions, editions, revisions, or other derivative works. This permission shall be effective as of the date of execution by the parties for the maximum period of 12 months and should be renewed after the term expires.
    i. When content is to be republished in a book or journal the validity of this agreement should be the life of the book edition or journal issue.
    ii. When content is licensed for use on a website, internet, intranet, or any publicly accessible site (not including a journal or book), you agree to remove the material from such site after 12 months, or request to renew your permission license
2. **Credit Line:** A credit line must be prominently placed and include: For book content: the author(s), title of book, edition, copyright holder, year of publication; For journal content: the author(s), titles of article, title of journal, volume number, issue number, inclusive pages and website URL to the journal page; If a journal is published by a learned society the credit line must include the details of that society.
3. **Warranties:** The requestor warrants that the material shall not be used in any manner which may be considered derogatory to the title, content, authors of the material, or to Wolters Kluwer Health, Inc.
4. **Indemnity:** You hereby indemnify and hold harmless Wolters Kluwer Health, Inc. and its respective officers, directors, employees and agents, from and against any and all claims, costs, proceeding or demands arising out of your unauthorized use of the Licensed Material
5. **Geographical Scope:** Permission granted is non-exclusive and is valid throughout the world in the English language and the languages specified in the license.
6. **Copy of Content:** Wolters Kluwer Health, Inc. cannot supply the requestor with the original artwork, high-resolution images, electronic files or a clean copy of content.
7. **Validity:** Permission is valid if the borrowed material is original to a Wolters Kluwer Health, Inc. imprint (J.B Lippincott, Lippincott-Raven Publishers, Williams & Wilkins, Lea & Febiger, Harwal, Rapid Science, Little Brown & Company, Harper & Row Medical, American Journal of Nursing Co, and Urban & Schwarzenberg - English Language, Raven Press, Paul Hoeber, Springhouse, Ovid), and the Anatomical Chart Company
8. **Third Party Material:** This permission does not apply to content that is credited to publications other than Wolters Kluwer Health, Inc. or its Societies. For images credited to non-Wolters Kluwer Health, Inc. books or journals, you must obtain permission from the source referenced in the figure or table legend or credit line before making any use of the image(s), table(s) or other content.
9. **Adaptations:** Adaptations are protected by copyright. For images that have been adapted, permission must be sought from the rightsholder of the original material and the rightsholder of the adapted material.
10. **Modifications:** Wolters Kluwer Health, Inc. material is not permitted to be modified or adapted without written approval from Wolters Kluwer Health, Inc. with the exception of text size or color. The adaptation should be credited as follows: Adapted with permission from Wolters Kluwer Health, Inc.: [the author(s), title of book, edition, copyright holder, year of publication] or [the author(s), titles of article, title of journal, volume number, issue number, inclusive pages and website URL to the journal page].
11. **Full Text Articles:** Republication of full articles in English is prohibited.
12. **Branding and Marketing:** No drug name, trade name, drug logo, or trade logo can be included on the same page as material borrowed from *Diseases of the Colon & Rectum, Plastic Reconstructive Surgery, Obstetrics & Gynecology (The Green*

Heart Association publications and the American Academy of Neurology publications.

13. **Open Access:** Unless you are publishing content under the same Creative Commons license, the following statement must be added when reprinting material in Open Access journals: "The Creative Commons license does not apply to this content. Use of the material in any format is prohibited without written permission from the publisher, Wolters Kluwer Health, Inc. ██████████████████████████ ████████████████

14. **Translations:** The following disclaimer must appear on all translated copies: Wolters Kluwer Health, Inc. and its Societies take no responsibility for the accuracy of the translation from the published English original and are not liable for any errors which may occur.

15. **Published Ahead of Print (PAP):** Articles in the PAP stage of publication can be cited using the online publication date and the unique DOI number.
    i. Disclaimer: Articles appearing in the PAP section have been peer-reviewed and accepted for publication in the relevant journal and posted online before print publication. Articles appearing as PAP may contain statements, opinions, and information that have errors in facts, figures, or interpretation. Any final changes in manuscripts will be made at the time of print publication and will be reflected in the final electronic version of the issue. Accordingly, Wolters Kluwer Health, Inc., the editors, authors and their respective employees are not responsible or liable for the use of any such inaccurate or misleading data, opinion or information contained in the articles in this section.

16. **Termination of Contract:** Wolters Kluwer Health, Inc. must be notified within 90 days of the original license date if you opt not to use the requested material.

17. **Waived Permission Fee:** Permission fees that have been waived are not subject to future waivers, including similar requests or renewing a license.

18. **Contingent on payment:** You may exercise these rights licensed immediately upon issuance of the license, however until full payment is received either by the publisher or our authorized vendor, this license is not valid. If full payment is not received on a timely basis, then any license preliminarily granted shall be deemed automatically revoked and shall be void as if never granted. Further, in the event that you breach any of these terms and conditions or any of Wolters Kluwer Health, Inc.'s other billing and payment terms and conditions, the license is automatically revoked and shall be void as if never granted. Use of materials as described in a revoked license, as well as any use of the materials beyond the scope of an unrevoked license, may constitute copyright infringement and publisher reserves the right to take any and all action to protect its copyright in the materials.

19. **STM Signatories Only:** Any permission granted for a particular edition will apply to subsequent editions and for editions in other languages, provided such editions are for the work as a whole in situ and do not involve the separate exploitation of the permitted illustrations or excerpts. Please view: STM Permissions Guidelines

20. **Warranties and Obligations:** LICENSOR further represents and warrants that, to the best of its knowledge and belief, LICENSEE's contemplated use of the Content as represented to LICENSOR does not infringe any valid rights to any third party.

21. **Breach:** If LICENSEE fails to comply with any provisions of this agreement, LICENSOR may serve written notice of breach of LICENSEE and, unless such breach is fully cured within fifteen (15) days from the receipt of notice by LICENSEE, LICENSOR may thereupon, at its option, serve notice of cancellation on LICENSEE, whereupon this Agreement shall immediately terminate.

22. **Assignment:** License conveyed hereunder by the LICENSOR shall not be assigned or granted in any manner conveyed to any third party by the LICENSEE without the consent in writing to the LICENSOR.

this Agreement and all rights and liabilities arising hereunder.

24. **Unlawful:** If any provision of this Agreement shall be found unlawful or otherwise legally unenforceable, all other conditions and provisions of this Agreement shall remain in full force and effect.

For Copyright Clearance Center / RightsLink Only:

1. **Service Description for Content Services:** Subject to these terms of use, any terms set forth on the particular order, and payment of the applicable fee, you may make the following uses of the ordered materials:
   i. **Content Rental:** You may access and view a single electronic copy of the materials ordered for the time period designated at the time the order is placed. Access to the materials will be provided through a dedicated content viewer or other portal, and access will be discontinued upon expiration of the designated time period. An order for Content Rental does not include any rights to print, download, save, create additional copies, to distribute or to reuse in any way the full text or parts of the materials.
   ii. **Content Purchase:** You may access and download a single electronic copy of the materials ordered. Copies will be provided by email or by such other means as publisher may make available from time to time. An order for Content Purchase does not include any rights to create additional copies or to distribute copies of the materials

Other Terms and Conditions:

v1.18

ELSEVIER LICENSE
TERMS AND CONDITIONS

Nov 14, 2020

This Agreement between ██████████████████ and Elsevier ("Elsevier") consists of your license details and the terms and conditions provided by Elsevier and Copyright Clearance Center.

License Number	4947461069177
License date	Nov 14, 2020
Licensed Content Publisher	Elsevier
Licensed Content Publication	Urology
Licensed Content Title	Novel Biologic Model for Percutaneous Renal Surgery Learning and Training in the Laboratory
Licensed Content Author	████████████████████████
Licensed Content Date	Sep 1, 2008
Licensed Content Volume	72
Licensed Content Issue	3
Licensed Content Pages	4
Start Page	513
End Page	516

Type of Use	reuse in a thesis/dissertation
Portion	figures/tables/illustrations
Number of figures/tables/illustrations	10
Format	both print and electronic
Are you the author of this Elsevier article?	No
Will you be translating?	No
Title	DEVELOPMENT AND VALIDATION OF AUGMENTED REALITYTRAINING SIMULATOR FOR ULTRASOUND GUIDEDPERCUTANEOUS RENAL ACCESS
Institution name	Western University
Expected presentation date	Nov 2020
Portions	fig 1,2,4
Requestor Location	
Publisher Tax ID	GB 494 6272 12
Total	0.00 USD
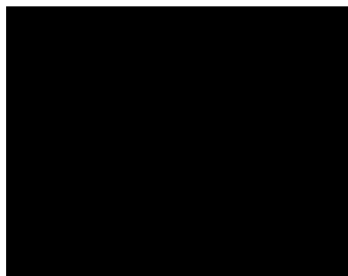
Terms and Conditions

materials.

9. Warranties: Publisher makes no representations or warranties with respect to the licensed material.

10. Indemnity: You hereby indemnify and agree to hold harmless publisher and CCC, and their respective officers, directors, employees and agents, from and against any and all claims arising out of your use of the licensed material other than as specifically authorized pursuant to this license.

11. No Transfer of License: This license is personal to you and may not be sublicensed, assigned, or transferred by you to any other person without publisher's written permission.

12. No Amendment Except in Writing: This license may not be amended except in a writing signed by both parties (or, in the case of publisher, by CCC on publisher's behalf).

13. Objection to Contrary Terms: Publisher hereby objects to any terms contained in any purchase order, acknowledgment, check endorsement or other writing prepared by you, which terms are inconsistent with these terms and conditions or CCC's Billing and Payment terms and conditions. These terms and conditions, together with CCC's Billing and Payment terms and conditions (which are incorporated herein), comprise the entire agreement between you and publisher (and CCC) concerning this licensing transaction. In the event of any conflict between your obligations established by these terms and conditions and those established by CCC's Billing and Payment terms and conditions, these terms and conditions shall control.

14. Revocation: Elsevier or Copyright Clearance Center may deny the permissions described in this License at their sole discretion, for any reason or no reason, with a full refund payable to you. Notice of such denial will be made using the contact information provided by you. Failure to receive such notice will not alter or invalidate the denial. In no event will Elsevier or Copyright Clearance Center be responsible or liable for any costs, expenses or damage incurred by you as a result of a denial of your permission request, other than a refund of the amount(s) paid by you to Elsevier and/or Copyright Clearance Center for denied permissions.

LIMITED LICENSE

The following terms and conditions apply only to specific license types:

15. **Translation**: This permission is granted for non-exclusive world **English** rights only unless your license was granted for translation rights. If you licensed translation rights you may only translate this content into the languages you requested. A professional translator must perform all translations and reproduce the content word for word preserving the integrity of the article.

16. **Posting licensed content on any Website**: The following terms and conditions apply as follows: Licensing material from an Elsevier journal: All content posted to the web site must maintain the copyright information line on the bottom of each image; A hyper-text must be included to the Homepage of the journal from which you are licensing at http://www.sciencedirect.com/science/journal/xxxxx or the Elsevier homepage for books at http://www.elsevier.com; Central Storage: This license does not include permission for a scanned version of the material to be stored in a central repository such as that provided by Heron/XanEdu.

homepage at http://www.elsevier.com . All content posted to the web site must maintain the copyright information line on the bottom of each image.

Posting licensed content on Electronic reserve: In addition to the above the following clauses are applicable: The web site must be password-protected and made available only to bona fide students registered on a relevant course. This permission is granted for 1 year only. You may obtain a new license for future website posting.

17. **For journal authors:** the following clauses are applicable in addition to the above:

Preprints:

A preprint is an author's own write-up of research results and analysis, it has not been peer-reviewed, nor has it had any other value added to it by a publisher (such as formatting, copyright, technical enhancement etc.).

Authors can share their preprints anywhere at any time. Preprints should not be added to or enhanced in any way in order to appear more like, or to substitute for, the final versions of articles however authors can update their preprints on arXiv or RePEc with their Accepted Author Manuscript (see below).

If accepted for publication, we encourage authors to link from the preprint to their formal publication via its DOI. Millions of researchers have access to the formal publications on ScienceDirect, and so links will help users to find, access, cite and use the best available version. Please note that Cell Press, The Lancet and some society-owned have different preprint policies. Information on these policies is available on the journal homepage.

Accepted Author Manuscripts: An accepted author manuscript is the manuscript of an article that has been accepted for publication and which typically includes author-incorporated changes suggested during submission, peer review and editor-author communications.

Authors can share their accepted author manuscript:

- immediately
    - via their non-commercial person homepage or blog
    - by updating a preprint in arXiv or RePEc with the accepted manuscript
    - via their research institute or institutional repository for internal institutional uses or as part of an invitation-only research collaboration work-group
    - directly by providing copies to their students or to research collaborators for their personal use
    - for private scholarly sharing as part of an invitation-only work group on commercial sites with which Elsevier has an agreement
- After the embargo period
    - via non-commercial hosting platforms such as their institutional repository
    - via commercial sites with which Elsevier has an agreement

In all cases accepted manuscripts should:

- link to the formal publication via its DOI
- bear a CC-BY-NC-ND license - this is easy to do
- if aggregated with other manuscripts, for example in a repository or other site, be shared in alignment with our hosting policy not be added to or enhanced in any way to

Published journal article (JPA): A published journal article (PJA) is the definitive final record of published research that appears or will appear in the journal and embodies all value-adding publishing activities including peer review co-ordination, copy-editing, formatting, (if relevant) pagination and online enrichment.

Policies for sharing publishing journal articles differ for subscription and gold open access articles:

<u>**Subscription Articles:**</u> If you are an author, please share a link to your article rather than the full-text. Millions of researchers have access to the formal publications on ScienceDirect, and so links will help your users to find, access, cite, and use the best available version.

Theses and dissertations which contain embedded PJAs as part of the formal submission can be posted publicly by the awarding institution with DOI links back to the formal publications on ScienceDirect.

If you are affiliated with a library that subscribes to ScienceDirect you have additional private sharing rights for others' research accessed under that agreement. This includes use for classroom teaching and internal training at the institution (including use in course packs and courseware programs), and inclusion of the article for grant funding purposes.

<u>**Gold Open Access Articles:**</u> May be shared according to the author-selected end-user license and should contain a [CrossMark logo](#), the end user license, and a DOI link to the formal publication on ScienceDirect.

Please refer to Elsevier's [posting policy](#) for further information.

18. **For book authors** the following clauses are applicable in addition to the above: Authors are permitted to place a brief summary of their work online only. You are not allowed to download and post the published electronic version of your chapter, nor may you scan the printed edition to create an electronic version. **Posting to a repository:** Authors are permitted to post a summary of their chapter only in their institution's repository.

19. **Thesis/Dissertation**: If your license is for use in a thesis/dissertation your thesis may be submitted to your institution in either print or electronic form. Should your thesis be published commercially, please reapply for permission. These requirements include permission for the Library and Archives of Canada to supply single copies, on demand, of the complete thesis and include permission for Proquest/UMI to supply single copies, on demand, of the complete thesis. Should your thesis be published commercially, please reapply for permission. Theses and dissertations which contain embedded PJAs as part of the formal submission can be posted publicly by the awarding institution with DOI links back to the formal publications on ScienceDirect.

<u>**Elsevier Open Access Terms and Conditions**</u>

You can publish open access with Elsevier in hundreds of open access journals or in nearly 2000 established subscription journals that support open access publishing. Permitted third party re-use of these open access articles is defined by the author's choice of Creative Commons user license. See our [open access license policy](#) for more information.

Terms & Conditions applicable to all Open Access articles published with Elsevier:

article nor should the article be modified in such a way as to damage the author's honour or reputation. If any changes have been made, such changes must be clearly indicated.

The author(s) must be appropriately credited and we ask that you include the end user license and a DOI link to the formal publication on ScienceDirect.

If any part of the material to be used (for example, figures) has appeared in our publication with credit or acknowledgement to another source it is the responsibility of the user to ensure their reuse complies with the terms and conditions determined by the rights holder.

Additional Terms & Conditions applicable to each Creative Commons user license:

CC BY: The CC-BY license allows users to copy, to create extracts, abstracts and new works from the Article, to alter and revise the Article and to make commercial use of the Article (including reuse and/or resale of the Article by commercial entities), provided the user gives appropriate credit (with a link to the formal publication through the relevant DOI), provides a link to the license, indicates if changes were made and the licensor is not represented as endorsing the use made of the work. The full details of the license are available at http://creativecommons.org/licenses/by/4.0.

CC BY NC SA: The CC BY-NC-SA license allows users to copy, to create extracts, abstracts and new works from the Article, to alter and revise the Article, provided this is not done for commercial purposes, and that the user gives appropriate credit (with a link to the formal publication through the relevant DOI), provides a link to the license, indicates if changes were made and the licensor is not represented as endorsing the use made of the work. Further, any new works must be made available on the same conditions. The full details of the license are available at http://creativecommons.org/licenses/by-nc-sa/4.0.

CC BY NC ND: The CC BY-NC-ND license allows users to copy and distribute the Article, provided this is not done for commercial purposes and further does not permit distribution of the Article if it is changed or edited in any way, and provided the user gives appropriate credit (with a link to the formal publication through the relevant DOI), provides a link to the license, and that the licensor is not represented as endorsing the use made of the work. The full details of the license are available at http://creativecommons.org/licenses/by-nc-nd/4.0. Any commercial reuse of Open Access articles published with a CC BY NC SA or CC BY NC ND license requires permission from Elsevier and will be subject to a fee.

Commercial reuse includes:

- Associating advertising with the full text of the Article
- Charging fees for document delivery or access
- Article aggregation
- Systematic distribution via e-mail lists or share buttons

Posting or linking by commercial companies for use by customers of those companies.

20. **Other Conditions**:

v1.10

Sent: Monday, November 16, 2020 11:02 AM
Subject: RE: Permission to Use Copyrighted Material in a Master's Thesis

Copyright Permission is granted for the inclusion of the requested article in your Master's thesis. Please give proper credit to the journal and the publisher.

Kind regards,

Mary Ann Liebert, Inc.
New Rochelle, NY

Subject: Permission to Use Copyrighted Material in a Master's Thesis

I am a University of Western Ontario graduate student completing my Master's thesis entitled "DEVELOPMENT AND VALIDATION OF AUGMENTED REALITYTRAINING SIMULATOR FOR ULTRASOUND GUIDEDPERCUTANEOUS RENAL ACCESS". My thesis will be available in full-text on the internet for reference, study and / or copy. Except in situations where a thesis is under embargo or restriction, the electronic version will be accessible through the Western Libraries web pages, the Library's web catalogue, and also through web search engines. I will also be granting Library and Archives Canada and ProQuest/UMI a non-exclusive license to reproduce, loan, distribute, or sell single copies of my thesis by any means and in any form or format. These rights will in no way restrict republication of the material in any other form by you or by others authorized by you.

I would like permission to allow inclusion of the following material in my thesis:

FIG. 1. Degrees of movement for tilt and rainbow.
Title: The SimPORTAL Fluoro-Less C-Arm Trainer: An Innovative Device for Percutaneous Kidney Access
Author: Domenico Veneziano, MD, FEBU, Arthur Smith, MD,Troy Reihsen, Jason Speich, and Robert M. Sweet, MD, FACS
Publication: Journal of Endourology
Publisher: Mary Ann Liebert, Inc.
Date: Feb 1, 2015

The material will be attributed through a citation.
Please confirm in writing or by email that these arrangements meet with your approval.

Curriculum Vitae

Name: Yanyu Mu

Post-Secondary   MESc, Biomedical Engineering
Education and   Western University, London, Ontario
Degrees: 2019 - Present

BESc, Electrical Engineering - Biomedical signals and systems
Western University, London, Ontario
2018

Related Work   Teaching Assistant
Experience: The University of Western Ontario
2018 - 2020

Research Assistant
The University of Western Ontario
2017 - 2018

Service Technician
Canadian Measurement Metrology
2014 - 2017

Service Technician
Industrial Drive Service Inc.
2013 - 2014

Journal Manuscript:

Mu, Y., Hocking, D., Wang, Z., Garvin, G.J., Eagleson, R. and Peters, T.M., Augmented reality simulator for ultrasound-guided percutaneous renal access. *International Journal of Computer Assisted Radiology and Surgery*, 15(5):749–757, 2020.

Abstracts:

Rivero, M., **Mu, Y.**, Roth, J., Wilson, T., Eagleson, R., and Sandig, M., Studying histology in 3d: Development and evaluation of an interactive virtual histologylearning tool using a 3d model of the renal corpuscle. *The FASEB Journal*, 32(S1):25.5–25.5, 2018.

Wang, Z., **Mu, Y.**, Hocking, D., Eagleson, R. and Peters, T.M., Augmented reality simulator for ultrasound guided percutaneous renal. *Journal of Urology*, 203(Supplement 4):e691–e692, 2020.

M. Sandig, J. Roth, M. Rivero, R. Tarbell, **Y. Mu**, R. Eagleson, and T. D. Wilson. Isteaching histology in 3d useful? volume 236, pages 45–45. WILEY 111 RIVER ST,HOBOKEN 07030-5774, NJ USA